



Iron oxide nanoparticles and their pharmaceutical applications



Nour F. Attia^{a,*}, Eman M. Abd El-Monaem^b, Hisham G. El-Aqapa^b, Sally E.A. Elashery^c, Abdelazeem S. Eltaweil^b, Misara El Kady^d, Shaden A.M. Khalifa^e, Hamada B. Hawash^f, Hesham R. El-Seedi^{g,h,i}

^a Chemistry Division, National Institute of Standards, 136, Giza 12211, Egypt

^b Chemistry Department, Faculty of Science, Alexandria University, Alexandria, Egypt

^c Chemistry Department, Faculty of Science, Cairo University, Gamaa Str., 12613, Giza, Egypt

^d Chemistry Department, Faculty of Science, Ain Shams University, Cairo, Egypt

^e Department of Molecular Biosciences, the Wenner-Gren Institute, Stockholm University, Stockholm SE-106 91, Sweden

^f Environmental Division, National Institute of Oceanography and Fisheries (NIOF), Kayet Bey, El-Anfoushy, Alexandria, Egypt

^g Pharmacognosy Group, Department of Pharmaceutical Biosciences, Uppsala University, Biomedical Centre, Box 591, 751 24, Uppsala, Sweden

^h Department of Chemistry, Faculty of Science, Menoufia University, Shebin El-Kom 32512, Egypt

ⁱ International Research Center for Food Nutrition and Safety, Jiangsu University, Zhenjiang 212013, China

ARTICLE INFO

Keywords:

Iron oxide nanoparticles

Anticancer

Antivirus

Synthesis routes

Antibacterial

Pharmaceutical applications

ABSTRACT

The importance of different polymorphic forms of iron oxide nanoparticles attracted a lot of attentions in various applications due to their unique electrical, optical and magnetic properties. Moreover, the excellent biocompatibility, high surface area, spherical shape, tunable nanoscale size and the availability of synthesis route make them desirable in various biological and pharmaceutical applications. To this aim, in this review, different synthesis methods of iron oxide nanoparticles were discussed, also the main characterization techniques used for elucidation of the iron oxide nanoparticles were reviewed. The exploitation of iron oxide nanoparticles-based systems as anticancer, antiviral, antimicrobial agents and its involvement in drug delivery system were reviewed in details. Additionally, the influence of nanoparticles size and the reagent type and conditions utilized in synthesis and their pharmaceutical applications was highlighted.

1. Introduction

Owing to the superior characteristics of the bountiful types of iron oxides nanoparticles (IONPs), they have drawn prominence in various applications facilitating the easy progress in high-technology based on nanoscale materials. The IONPs exist in various forms based on their different phases such as magnetite, hematite, maghemite and wustite [1]. However, the main forms of IONPs used are γ -Fe₂O₃, α -Fe₂O₃ and Fe₃O₄ due to their unique features and physiochemical properties [1]. Interestingly, the existence of IONPs in nanoscale creates new features to the materials such as outstanding magnetic, electrical and optical properties which is responsible to the quantum size phenomena [2–4]. It was noticed that the more the IONPs size decreases, the more their superparamagnetic behavior will be improved in contrast to the ferromagnetic behavior that will decline [5]. Interestingly, the (10–20 nm) size of IONPs reflects good superparamagnetic properties of Fe₃O₄ and γ -Fe₂O₃ and hence, significant performance in various applications.

Interestingly, due to the promising biocompatibility, high stability, biodegradability, nontoxicity and low cost of preparation IONPs can be used for variety of pharmaceutical applications [21] including electronics [6], energy [7], biomedicine [8], biotechnology [9] and agriculture [10]. Our group has long been involved in the synthesis and applications of various nanoscale materials [11–20]. Thus, in this review the recent progress of exploitation of IONPs in pharmaceutical application will be reviewed and discussed.

2. Synthesis of IONPs

The high efficiency of IONPs is owned to the physical and chemical characteristics including nanoscale dimensions with spherical shape and tunable size of less than 50 nm (\sim 35 nm), in addition to the large surface area and superparamagnetic properties [21–23]. Interestingly, IONPs can be synthesized using various approaches, where each method can produce particular features of shape, size, distribution, chemical

* Corresponding author.

E-mail addresses: drnour2005@yahoo.com (N.F. Attia), sally_elsayed_ahmeda@cu.edu.eg (S.E.A. Elashery).

stability and superparamagnetic powers. The most commonly used method is co-precipitation method [24], and in general, the synthesis of IONPs can be classified into three main approaches: chemical, physical and green synthesis methods as reviewed in schematic diagram depicted in Fig. 1. Additionally, these methods have been thoroughly reviewed and reported in recent report [24]. Thus, various chemical methods have been reported for synthesis of IONPs such as co-precipitation [25–27], sol-gel [28–32], sonochemical [33–35], thermal decomposition technique [36–39], microemulsion [26,40–43], hydrothermal [24,44–47] and polyols [48–52]. This is in addition to a variety of physical methods including ball milling [53–56], gas-phase deposition [57,58], pulsed-laser ablation [59–61] and green synthesis [62–64]. We and others dedicated researches for development of IONPs for various applications and development of sensors and adsorbents for determination and recovery of iron ions [65–88].

3. Iron oxide nanoparticles for pharmaceutical applications

3.1. Iron oxide nanoparticles as anticancer agents

Mousavi et al. [89] studied the anticancer activity of kombucha modified Polyrhodanine/Fe₃O₄/graphene oxide nanocomposite (PR/GO/Fe₃O₄/KO) against hepatocarcinoma (Hep-G2) cell line. The study findings suggested the high sensitivity of PR/GO/Fe₃O₄/KO to detect the target cell within biological fluids. Interestingly, the cytotoxicity study of Hep-G2 after being treated with different concentration of Fe₃O₄, PR/Fe₃O₄, PR/GO/Fe₃O₄, PR/GO/Fe₃O₄/KO, PR/Fe₃O₄/KO, and GO/Fe₃O₄ was executed. In agreement with Markides et al. [90] and Gholam et al. [91] studies, Fe₃O₄ has no cytotoxicity against Hep-G2 cell lines in the above mentioned study since the cell viability declined from 132 to 88% in response to the increase in Fe₃O₄ concentration from 1 to 500 µg/mL, respectively. However, the high concentration of PR/Fe₃O₄ led to a dramatic diminution in Hep-G2 viability reached 44% which may be explained by the high cytotoxicity of the pure PR [92]. Furthermore, PR/GO/Fe₃O₄ has more cytotoxicity than Fe₃O₄/GO which is expected as several studies reported that Fe₃O₄/GO are well

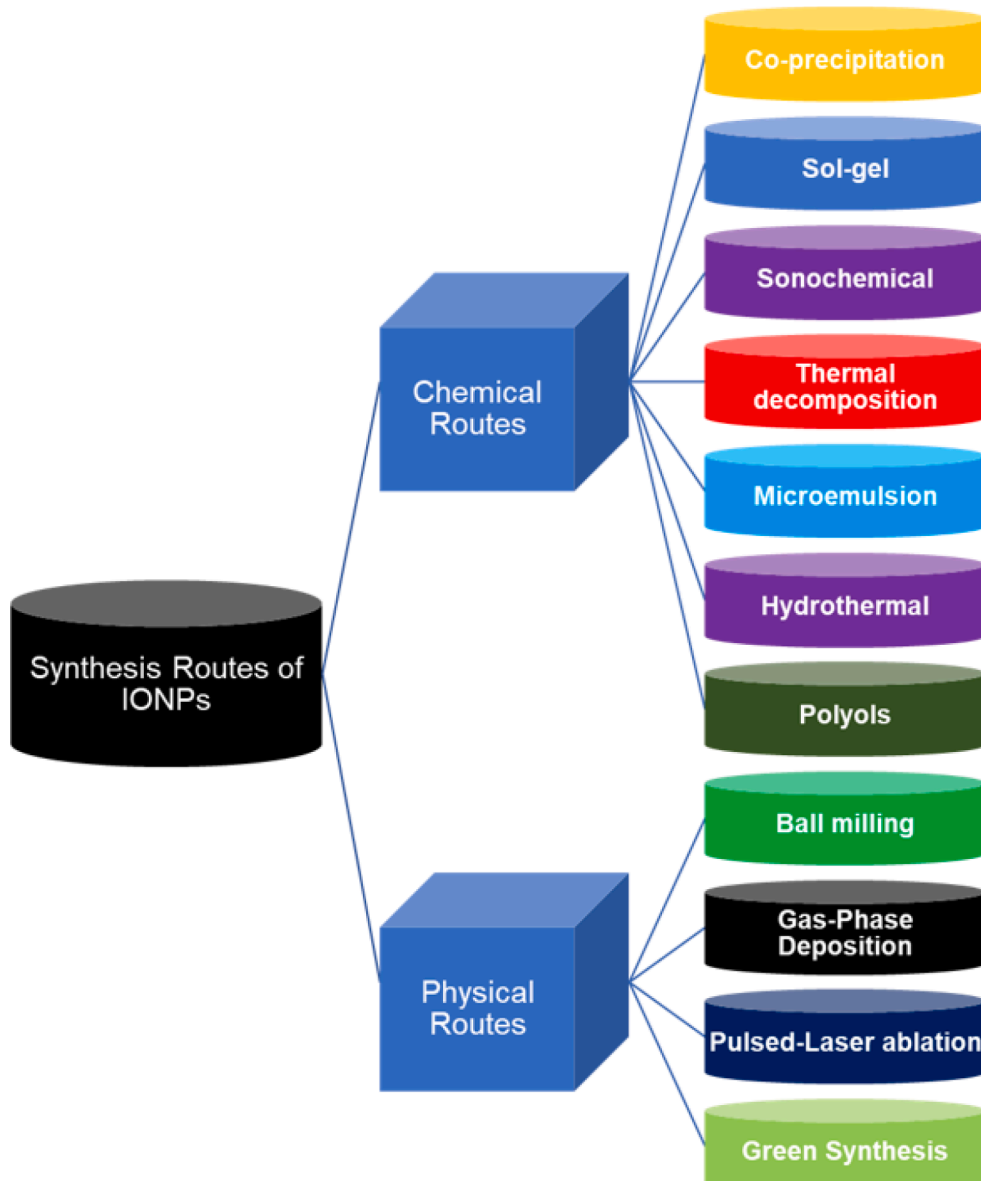


Fig. 1. Schematic diagram representing the different routes for synthesis of IONPs.

tolerated by animal and human cell lines [93].

In another study, Jana et al. [94] tested α -Fe₂O₃-ZnO composite as antitumor against MCF-7 and Hep-G2 cells, employing MTT assay on them. An augmentation in the cytotoxicity from 30 to 90% was monitored following the rise of the α -Fe₂O₃-ZnO concentration from 50 to 250 μ g/mL. This finding was in line with Malaikozhundan et al. study that depicted the ability of the higher ZnO concentration to inhibit the growth of MCF-7 cell7 (a breast cancer cell line) [95]. Equally important, Siddiqui et al. study has evinced the copper oxide concentration-dependent cytotoxicity of HepG2 cells [96]. The higher toxicity with the increase of α -Fe₂O₃-ZnO concentration was evidential, supporting the notion that the availability of large numbers of the particles is to facilitate their attachment to the cancerous cells, rupture their membranes, enter into the cytoplasm, and destroy cellular organelles utilizing the reactive oxygen species (ROS).

Izadiyan et al. [97] evaluated the anticancer effect of Fe₃O₄/Au nanoparticles on NIH-3T3 (mouse cell lines) and HT-29 (human colorectal cell lines). It was observed that inhibitory concentration (IC₅₀) could not be achieved for the normal cell whether from human or mouse even if the Fe₃O₄/Au concentration exceeded 500 μ g/mL. In the meanwhile, Fe₃O₄/Au elucidated a toxicity on the colorectal cancer cell line, HT-29 and the estimated IC₅₀ reached 235 μ g/mL. This result is in line with Gholoobi et al. [98] findings that cancerous cervical cell lines well tolerated starch coated Fe₃O₄ nanoparticles in *in vitro* cytotoxicity assay. On the other hand, it was found from microscope images that Fe₃O₄/Au nanoparticles with HT-29, resulted in a remarkable cell death. Notably, NIH-3T3 cell lines still have the fibroblast morphology in a vital state.

Similarly, Yew et al. [99] assessed the anticancer activity of MMT/SW/Fe₃O₄ with (MMT refers to montmorillonite and SW refers to the seaweed *Kappaphycus Alvarezii*) and without protocatechuic acid (PCA) drug against cancerous colorectal (HCT116) and normal colon (CCD112) cell lines. It was found that the killing activity of MMT/SW/Fe₃O₄ and MMT/SW/Fe₃O₄-PCA toward HCT116 cell is superior compared to CCD112 cell, reflecting the selectivity of both nanocomposite towards the cancerous cell lines. Hence, when the cells treated by 0.5 mg/mL MMT/SW/Fe₃O₄, the cell death of HCT116 significantly reached 70%, whereas the viability of CCD112 cells is still almost 100%. 1 mg/mL MMT/SW/Fe₃O₄-PCA killed 75% of HCT116 and 50% of CCD112, respectively. PCA exhibited the highest IC₅₀ (0.148 mg/mL) against HCT116, meanwhile, MMT/SW/Fe₃O₄ revealed higher IC₅₀ of 0.837 and 0.306 mg/mL against both CCD112 and HCT116, respectively, in comparison to MMT/SW/Fe₃O₄-PCA with IC₅₀ of 0.644 and 1 mg/mL against HCT116 and CCD112, respectively. Consequently, no synergistic anticancer activity was found when PCA combined to the MMT/SW/Fe₃O₄, as the MMT/SW/Fe₃O₄ exhibited superior anticancer action alone and also reflects suitability to be used as a nano carrier for cancer cell treatment. On the contrary, MMT/SW/Fe₃O₄ and MMT/SW/Fe₃O₄-PCA ruptured the cell membranes, resulting in cell death. This results were in disagreement with Barahuie et al. [100] and Saifullah et al. [101] studies where they demonstrated the excellent anticancer activity of PCA-loaded nanocomposites.

In another study, Ramalingam et al. [102] investigated the α -Fe₂O₃ as potential treatment for ovarian cancer (PA-1). The studied HRTEM (high resolution transmission electron microscope) showed that the fabricated α -Fe₂O₃ shape was not uniform where diverse shapes (hexagonal, spherical and triangle) were seen with a mean particles size around 28 nm. VSM (vibrating sample magnetometry) showed the ferromagnetic property of α -Fe₂O₃ with saturation magnetization of about 15 emu/g. This magnetic property of α -Fe₂O₃ facilitates the accumulation of the new compounds in cancer cells [103]. Besides, AFM (atomic force microscope) pointed out that the 2-D topography of α -Fe₂O₃ has irregular shape with less aggregation, uniform distribution and particles size < 35 nm. Moreover, MTT (3-(4,5-dimethylthiazol-2-yl)-2,5-diphenyltetrazolium bromide) tetrazolium reduction

assay showed the great ability of α -Fe₂O₃ to attenuate the growth of PA-1 cell lines. In addition, the cytotoxic activity on the cancerous PA-1 cell lines was < 20% with α -Fe₂O₃ concentration about 20 mg/mL. The microscope images pointed out a great change in the morphology of the control PA-1 after the treatment with α -Fe₂O₃ since the cells shape became irregular, enlarged and accumulated. This observation may be ascribed to the ability of α -Fe₂O₃ to suppress the colony-forming ability of PA-1 owing to the higher α -Fe₂O₃ inside the cells that established the higher cytotoxic activity, decreasing the survival rate of PA-1.

In another investigation, Saranya et al. [104] studied the anticancer activity of Fe₂O₃/Ag nanocomposite against lung cancer (A549 cell line). MMT assay pointed out the less cell viability of the treated cells compared to the control cells. It was found that Fe₂O₃/Ag with concentration 100-200 μ g/mL was nontoxic to A549. While, the increase in the Fe₂O₃/Ag concentration 300-400 μ g/mL showed strong decline in the A549 cell viability. However, the same concentration of pristine Fe₂O₃ exhibited less cytotoxicity to the cells. It was reported that the higher anticancer activity of Fe₂O₃/Ag compared to Fe₂O₃ may be attributed to the formation of ROS that destroy the breast cancer cells (MCF-7) [104]. Also, Fe₂O₃-Cu₂O-TiO₂ nanocomposite exhibited an excellent anticancer activity against MCF -7 at which it induced the cancerous cell apoptosis [105,106]. Fig. 2 (a-e) elucidated the change in the morphology of A549 with the raising in the Fe₂O₃/Ag concentration. Besides, there was interruption in the cytoskeleton of the treated cells and shrink in the membrane, confirming the anticancer activity of Fe₂O₃/Ag nanocomposite against A549 cell lines.

From that perspective, Vignesh et al. [107] studied the *in vitro* antitumor effect of exopolysaccharide-stabilized iron oxide nanoparticles (EPS-FeONPs) on epidermoid carcinoma cells (A431). It was found from the MTT assay that both EPS and EPS-FeONPs possessed a significant ability to inhibit the cancerous A431 cells growth in a dose-dependent manner. Furthermore, EPS-FeONPs revealed an advanced growth reduction at 24 h since IC₅₀ values of EPS and EPS-FeONPs were 350.18 and 62.946 mg/mL, respectively (Fig. 2f). Acridine orange/ethidium bromide (AO/EtBr) fluorescent staining was utilized to prove the A431 apoptosis (Fig. 2g). The control A431 cell lines showed a typical morphology that was confirmed by the uniform green fluorescence. While, the treated A431 cell lines with EPS-FeONPs revealed changes in the morphology such as cell shrinking, chromatin condensing and forming apoptotic bodies at 12 and 24 h. Several studies reported EPS as an anticancer, but its hydrophilic property and large size decreased the EPS uses in biomedical applications [108]. However, the combination between EPS and FeONPs exhibited an ameliorated activity and boosted bioavailability which may be attributed to the FeONPs properties as clarified from the cytotoxicity studies.

3.2. Iron oxide nanoparticles as antiviral agents

With the outbreak of several viral infectious diseases such as Ebola, Zika, Nipah, Influenza, coronavirus, etc., researchers have started to develop different types of antiviral agent-based nanomaterials to defeat the pathogens. Remarkably, with an excellent and tailorabile surface chemistry, colloidal stability, biodegradability, biocompatibility, and superparamagnetic property, IONPs have exhibited an excellent anti-viral potentiality against several viruses such as Influenza virus, HBV, HIV, and monkeypox virus in terms of irreversible damage of the viral genome, and inactivation of the viral genome replication [109,110]. However, the strong dipole-dipole interaction between particles, and agglomeration of pristine IONPs limited their workability in the biomedical applications [111]. Therefore, the ease of surface functionalization with polymeric capping agents could be a promising strategy that controls their agglomeration and ameliorates their biocompatibility and binding capability with the biomolecules. In this vein, the antiviral activity of PEG (polyethylene glycol) and PVP (polyvinylpyrrolidone) polymer-capped superparamagnetic Fe₃O₄, fabricated via simple polyol assisted solvothermal process was tested against H1N1 Influenza A virus

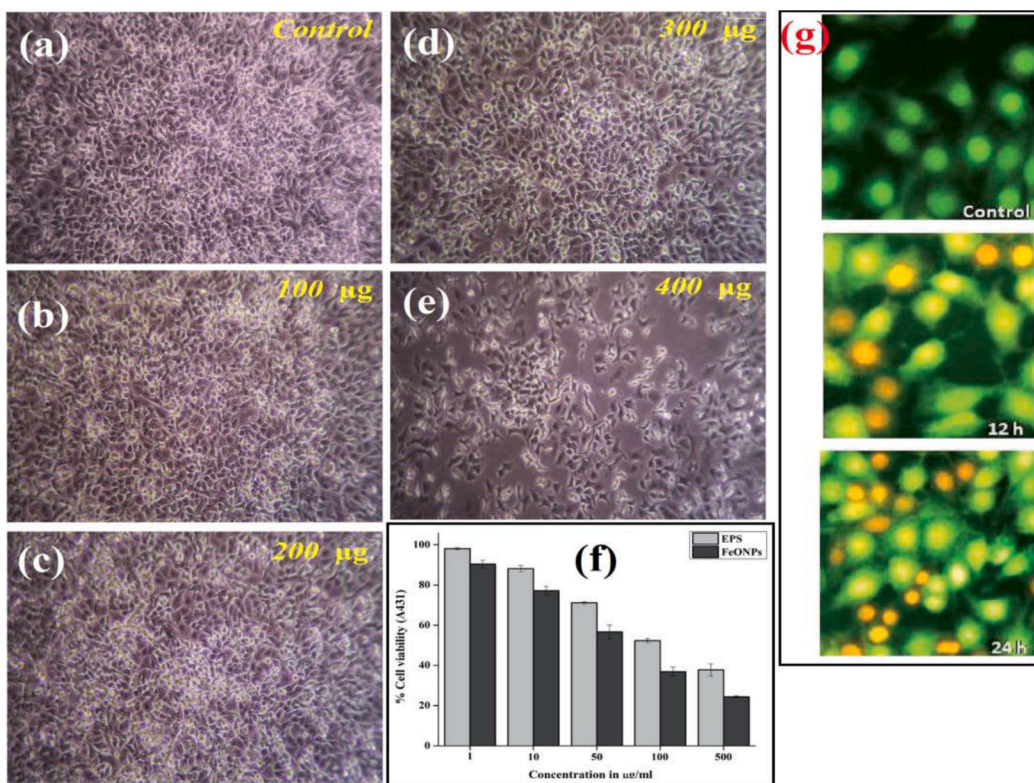


Fig. 2. The morphology of (a) control A549 cells and (b-e) treated A549 cells with various concentration of $\text{Fe}_3\text{O}_4/\text{Ag}$. Reproduced with permission [104]. Copyright 2020, Elsevier, (f) MMT assay and (g) AO/EtBr staining. Reproduced with permission [107]. Copyright 2015, RSC.

(Table 1) [112]. MTT assay of both PEG and PVP capped Fe_3O_4 NPs exhibited superior cell viabilities of 70% and 80%, respectively than the pristine magnetic NPs of 60% after 72h, confirming the improved biocompatibility of the magnetic NPs after surface capping. Moreover, PEG and PVP capped Fe_3O_4 NPs accomplished better virucidal effect against H1N1virus for MDCK cells comparable to the pristine Fe_3O_4 NPs which was verified through the cytopathic and virus yield reduction assay. Such higher viral inhibition accompanied with the polymer capped Fe_3O_4 NPs was attributed to the strong binding interaction between the surface of the capped nanoparticles and the glycoproteins of H1N1virus, thus inhibiting RNA replication, consequently the viral growth [113]. This mechanism was further verified via RT-PCR analysis that revealed a noticeable reduction of NP-RNA. Another study showed a potential antiviral activity against H1N1 Influenza A virus for glycine coated Fe_3O_4 NPs with particle size range of 10-15 nm (Table 1) [109]. Notably, the RT-PCR analysis exhibited 8-fold reductions in the viral existence after 24 h of viral infection in presence of IONPs. Such result was explained based on the binding interactions between the nanoparticles and -SH groups of the protein knobs of Influenza virus which in turn suppressed the proteins and retarded the viral growth [114]. Further, Bromberg et al. demonstrated an outstanding antiviral behavior of different types of silica coated magnetite nanoparticles functionalized with aziridine, poly(hexamethylene biguanide), or poly(ethyleneimine) (A-M/SiO_2 , PHMBG-M/ SiO_2 , or PEI-M/ SiO_2) core-shell nanostructures against various viral infectious pathogens such as bacteriophage MS2, herpes simplex virus (HSV-1), non-enveloped infectious pancreatic necrosis virus (IPNV), and enveloped viral hemorrhagic septicaemia virus (VHSV) (Table 1) [115]. Owing to the similar size, structure, and chemical composition of the bacteriophage MS2 to the human pathogenic enteroviruses such as poliovirus, bacteriophage MS2 was fully investigated as a mimic model [116,117]. The result exhibited an efficient removal of bacteriophage MS2 over 99% from an aqueous suspension with a reduction factor > 4 with a concentration range of

0.05-0.2 mg/ml of A-M/SiO_2 , PHMBG-M/ SiO_2 , and PEI-M/ SiO_2 particles. Actually, this remarkable virucidal efficiency was governed by different types of binding mechanisms. In fact, the electrostatic interaction between the positively charged surface of the nanoparticles and the negatively charged virions was the predominant binding interaction at pH range of 4-10 for the three antiviral agents [118]. Besides, the large numbers of hydrophobic methylene groups of PHMBG-M/ SiO_2 particles were responsible for the complexation between the surface of the nanoparticles and the amphiphilic virion protein coating. In addition, the antiviral activity of A-M/SiO_2 particles was attributed to the ionic binding between aziridine group and the negatively charged guanine nucleotide of the viral genome causing an inactivation of the DNA or RNA polymerase, and so inhibited the genome replication [119]. More importantly, the superparamagnetic property of Fe_3O_4 facilitated the separation of the virus-nanoparticles complex from the aquaculture, establishing their perfect antiviral applicability.

Recently, ferromagnetic NPs unveiled their mimetic peroxidase activity for the catalytic conversion of hydrogen peroxide into hydroxyl radical [120]. Unlike natural enzymes, the catalytic activity of IONs can be improved due to their versatile physico-chemical properties such as size, morphology, and ease of surface modulation. Qin T. and coworkers investigated the lipid peroxidation of the viral membrane envelope of Influenza A virus (IAV) as a powerful strategy for the viral eradication using a bio-inspired artificial enzyme (IONzyme) [121]. IONzyme achieved an excellent catalytic lipid peroxidation performance in neutral conditions, indicating its striking resemblance with lipoxidase rather than peroxidase that required acidic conditions. Notably, TEM images showed a vivid degradation of the lipid envelope as well as the neighboring proteins such as hemagglutinin, neuraminidase (NA), and matrix protein1 (M1) under high concentration of IONzyme (> 1 mg/mL). Clearly, there was an obvious relationship between the lipid envelope peroxidation and the destruction of the neighboring protein. Such finding was further confirmed via western blot analysis that showed a

noticeable destruction of a purified hemagglutinin protein using an IONzyme-liposome system. This result asserted the simultaneous destruction of the lipid envelope and proteins induced by the peroxidation process, thus vanishing the viral membrane, and so inactivating the virucidal effect. Efficiency of the IONzymes treated viral particles to infect the host cells was further tested using MDCK cells by examining attachment, proliferation and release of H5N1 viruses. As a result, the infectivity of H5N1 virus to the host cell was abolished by preventing the attachment step of the virus with the binding receptors of the host cell, prohibiting their entry into the cell and replication as depicted in Fig. 3. Interestingly, IONzymes showed a broad-spectrum antiviral activity against different subtypes of IAVs such as H1-H12 unveiling their anti-viral proficiency.

Considering the dire consequences that emerged for the outbreak of the COVID-19 pandemic, the medical staff and researchers have attempted to develop vaccines and antiviral therapeutics to combat such a catastrophic health problem. Recently, NPs offered an unprecedented antiviral activity owing to their biocompatibility that was approved by the FDA (food and drug administration) [122], and their strong interaction and passivation of several infectious diseases. IONs could be a promising antiviral candidate against SARS-CoV-2 virus that irreversibly bind to its spike proteins, causing inactivation for its viral activity and genome replication into the host cell. Abo-zeid et al. addressed an *in vitro* analysis, investigating the antiviral activity of both Fe_2O_3 and Fe_3O_4 against SARS-CoV-2 S1-RBD using molecular docking analysis (Table 1) [123]. Obviously, both Fe_2O_3 and Fe_3O_4 formed an efficient complexation with the spike protein of the virus (S1-RBD). However, according to the molecular docking analysis, Fe_3O_4 formed more stable complex than Fe_2O_3 due to the lower binding free energy. In fact, this efficient binding was presumably attributed to the conformational change of the protein structure, hindering the viral interaction with receptors of the host cell and their entry into it, and so prohibiting their proliferation.

3.3. Iron oxide nanoparticles as antimicrobial agents

Although, the evidential properties of iron oxide as antimicrobial, it

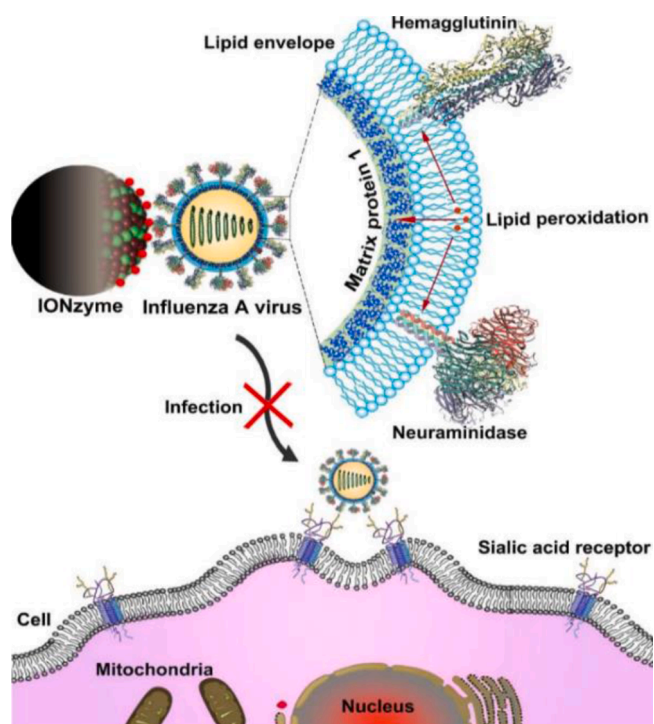


Fig. 3. Schematic of viral liperoxidation by IONzymes for virus inactivation [121].

suffers some flaws recognized as aggregation tendency, surface oxidation and the lack of functional groups. So, several studies have been executed to improve the iron oxide antimicrobial applications.

Linh Nguyen et al. [126] reported the efficiency of acrylic polyurethane/ Fe_3O_4 -Ag composite nanoparticles (ACPU/ Fe_3O_4 -Ag) as an antibacterial against (*Escherichia coli*) *E. coli* owing to the fast release of Ag^+ from the composite and the ionization of Ag accelerated by Fe^{3+} ions [127]. Besides, it was deduced that the incorporation of Ag into Fe_3O_4 inhibited the human cells toxicity by the free Ag [128]. FESEM (field emission scanning electron microscope) images of ACPU-/ Fe_3O_4 -Ag (Fig. 4a, b) clarified the well-dispersion of Fe_3O_4 -Ag without any agglomeration and the mean particles size of 10–20 nm. It was found that ACPU exhibited no inhibition for bacterial growth, inferring ACPU has poor bactericidal activity against *E. coli* (Fig. 4c). While ACPU/ Fe_3O_4 -Ag declined the growth rate of *E. coli* by the vicinity of 5% after 5 h of cultivation. This behavior may be ascribed to the excellent bactericidal activity of Fe_3O_4 -Ag owing to the super high catalytic activity of Ag and its good dispersion due to the Fe_3O_4 carrier. Moreover, there is a large surface area between ACPU/ Fe_3O_4 -Ag and the bacterial cell membrane [129].

In another study, Dacrory et al. [130] investigated the role of Fe_3O_4 in the enhancement of the antimicrobial activity of cyanoethyl cellulose (CEC) against G + ve (*Staphylococcus aureus*), G-ve (*Escherichia coli*), yeast (*Candida albicans*), and fungus (*Aspergillusniger*) using the agar plate process. The concrete results pointed out the propitious activity of CEC against *Staphylococcus*, *Escherichia coli*, and *Candida albicans* compared to *Aspergillusniger*. Furthermore, the raising in Fe_3O_4 dose (0.2–0.4 g) increased the zone of inhibition (ZOI), revealing the enhanced antimicrobial activities of CEC/ Fe_3O_4 composite films against G + ve, G -ve, yeast, and fungus compared to the pristine CEC. These propitious antimicrobial activities of CEC/ Fe_3O_4 films can be explained by the strong interaction between the negative membrane of the microbes and the positive metal, so the microbes oxidized and died. Besides, the generated ROS by Fe_3O_4 reacted with the thiol group of the protein, resulting in the formation of H_2O_2 . Consequently, Fe could react with H_2O_2 and form radicals that damage the membrane of the microbes [131,132].

In another investigation, Mirsadeghi et al. [133] studied the antimicrobial activity of Fe_3O_4 /Au nanocomposite against the pathogenic bacteria *E. coli*, *Bacillus* and *Estaphilu*. Fig. 4d depicted that Fe_3O_4 /Au even with low concentration possessed an excellent antimicrobial activity against the three pathogenic strains since the ZOI was at the range of 17–27 mm (Fig. 4e). Furthermore, the suggested mechanism of antimicrobial activity of Fe_3O_4 /Au against *E. coli*, *Bacillus* and *Estaphilu* occurred via the formation of an oxidative stress via OH^- , ROS, H_2O_2 and superoxide radicals (O_2^-), destroying the proteins and DNA in bacteria [134]. In a similar study, Lee et al. [135] reported that nanoparticles with a small particles size (10–80 nm) possess the ability to diffuse the bacterial membrane, resulting in antibacterial effects on bacterial strain. This was in line with, Rana et al. [136] that reported the efficacious antibacterial activity of pectin@ γ - Fe_2O_3 nanoparticles against *P. aerugenosa*, *S. aureus*, *B. cereus* and *S. typhii* occurred via the same mechanism. Moreover, the obtained result figured out that pectin@ γ - Fe_2O_3 possessed a promising antibacterial activity in particular against *S. aureus* and *S. typhii* at a concentration of 40 μL .

In another attempt, Arshad et al. (Table 2) [137] evaluated the antimicrobial activity of SiO_2 - Fe_2O_3 nanoparticles against *C. parapsilosis*, *A. niger*, *E. coli* and *B. subtilis* in different solvents. It was found that SiO_2 - Fe_2O_3 in acetonitrile was high aggregated into clusters owing to the dipole-dipole interactions between the particles with a diameter range of 38–40 nm. Also, the particles of SiO_2 - Fe_2O_3 in n-hexane were aggregated with a diameter range of 35–37 nm. While in isoamyl alcohol SiO_2 fused over the Fe_2O_3 surface and the mean particles size of SiO_2 - Fe_2O_3 was 51 nm. It was noticed that SiO_2 - Fe_2O_3 had an excellent inhibition against the four strains, depending on the solvent type.

Table 1

Summary of some modified magnetic NPs as antiviral agents.

Antiviral agents	Viruses	Particle sizes (nm)	Mechanism of action	Refs.
PEI-M/SiO ₂ A-M/SiO ₂ PHMBG-M/SiO ₂	Bacteriophage MS2	150-250	Electrostatic interaction between the positively charged surface of the nanoparticles and the negatively charged virions. Ionic binding between aziridine group and the negatively charged guanine nucleotide of the viral genome causing an inactivation of the DNA or RNA polymerase, and so inhibited the genome replication. Complexation between the surface of the nanoparticles due to the large numbers of methylene group and the amphiphilic virion protein coating.	[115]
Glycine coated Fe ₃ O ₄	H1N1 influenza A virus	10-15	Binding interactions between the nanoparticles and -SH groups of the protein knobs of Influenza virus which in turn suppressed the proteins and retarded the viral growth.	[109]
Fe ₂ O ₃ Fe ₃ O ₄	SARS-CoV-2	-	An efficient complexation with the spike protein of the virus (S1-RBD) causing conformational change of the protein structure, hindering the viral interaction with receptors of the host cell and their entry into it, and so prohibiting their proliferation.	[123]
IONzymes	H1N1 influenza A virus and its subtypes	-	Lipid peroxidation of the viral membrane envelope, preventing the attachment step of the virus with the binding receptors of the host cell, prohibiting their entry into the cell and replication.	[121]
PEG coated Fe ₃ O ₄ PVP coated Fe ₃ O ₄	H1N1 influenza A virus	20-30 10-15	Binding interaction between the surface of the capped nanoparticles and the glycoproteins of H1N1virus, thus inhibiting RNA replication, consequently the viral growth.	[112]
Maghemite (Fe ₂ O ₃ -NPs)	polio virus-1 polio virus-2	~ 10	N/A	[124]
Aptamer-functionalized MNPs	hepatitis C virus (HCV)	100	Interaction with the protein on the surface of HCV, then capture and concentration using a magnetocollection.	[125]

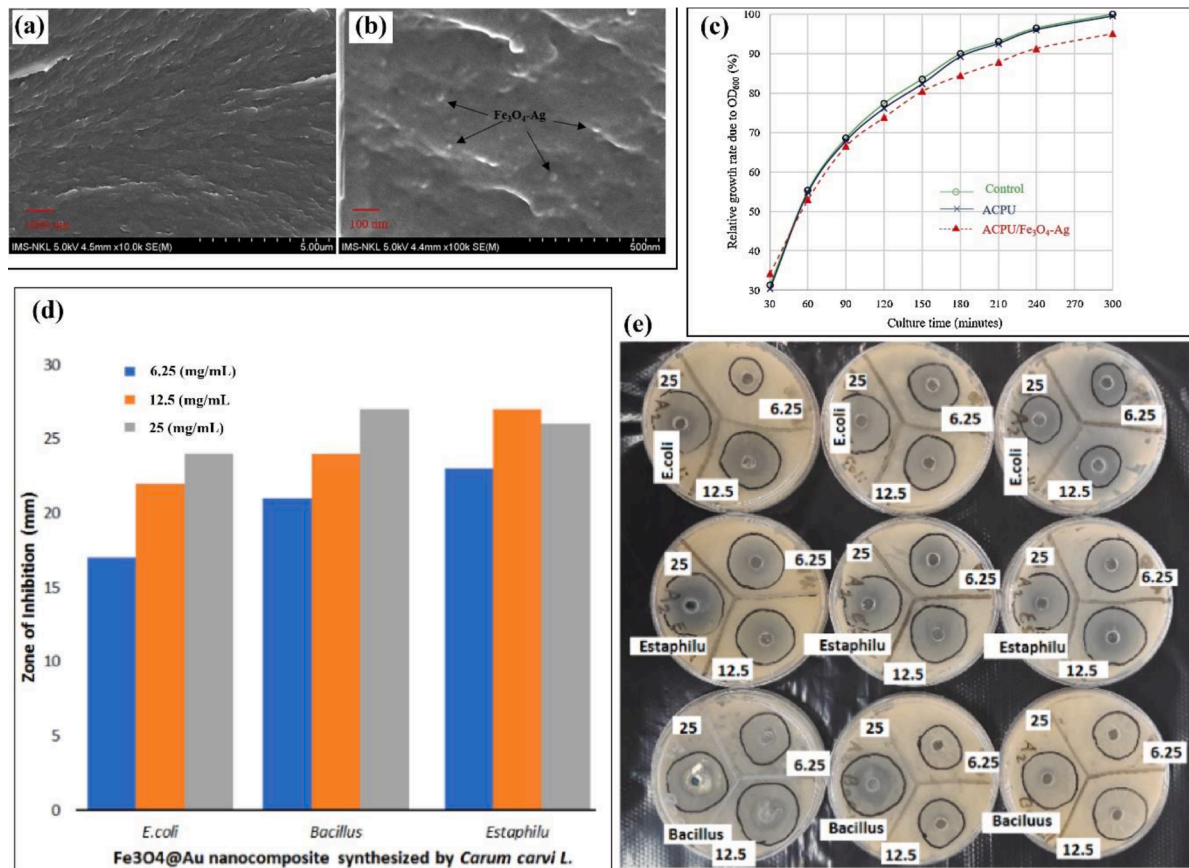


Fig. 4. (a, b) FESEM of ACPU/Fe₃O₄-Ag and (c) Effect of ACPU/Fe₃O₄-Ag on the growth rate of *E. coli*. Reproduced with permission [126] Copyright 2019, Elsevier, (d) The antimicrobial activity of Fe₃O₄/Au against *Estaphilu*, *Escherichia coli*, and *Bacillus subtilis* and (e) Digital photographs to ZOI. Reproduced with permission [133] Copyright 2020, Elsevier.

SiO₂-Fe₂O₃ exhibited the highest antifungal and antibacterial activities in acetonitrile since the minimum inhibitory concentration (MIC) values for *C. parapsilosis* and *A. niger* reached 0.31 and 0.21 mg/L, respectively. While the MIC values in isoamyl alcohol were 0.24 and 0.18 mg/L and in n-hexane were 0.09 mg/L for both strains.

In another study, Halliah et al. [138] synthesized α-Fe₂O₃/chitosan (α-Fe₂O₃/Cs) dip-coated on silk and cotton for inhabiting the growth of *E. coli* and *S. aureus* organisms. The antibacterial test revealed that α-Fe₂O₃/Cs coated fabrics had higher ZOI than α-Fe₂O₃ coated fabrics. Moreover, the ZOI increased with the increase in the concentration of

both α -Fe₂O₃/Cs coated fabrics and α -Fe₂O₃ coated fabrics. Also, GO-modified Fe₃O₄ nanocomposite (GO-Fe₃O₄) exhibited a great antibacterial potency against both G + ve (*S. aureus* and *B. Subtilis*) and G-ve pathogens (*P. aeruginosa* and *S. typhi*) [139]. The experimental results implied the ameliorated antibacterial effect of GO-Fe₃O₄ against all the tested bacteria compared to the pristine components. This result may be assigned to large surface area of GO-Fe₃O₄ that increase the contact with bacteria. Moreover, GO-Fe₃O₄ had greater antibacterial potency against G + ve than G-ve, at which G + ve does not possess the outer lipopolysaccharide membrane in its cell wall [140]. In one investigation, Siddiqui et al. (Table 2) [141] fabricated binary iron-zirconium oxide decorated black cumin seed (Fe₂O₃-ZrO₂/BC). The antibacterial activity of Fe₂O₃-ZrO₂/BC was studied against *E. coli* by measuring the ZOI. The test pointed out the significant antibacterial potency of Fe₂O₃-ZrO₂/BC towards *E. coli* since the measured ZOI was 25 mm. Moreover, the MIC value of Fe₂O₃-ZrO₂/BC for *E. coli* was 0.030 mg/mL, reflecting an advanced antibacterial potency compared with previous studies [142]. This finding may be attributed to the synergistic effect between BC seeds and Fe₂O₃-ZrO₂ at which they possessed superb phytogenic properties [143,144]. In addition, the ability of Fe₂O₃-ZrO₂/BC to penetrate into the cell membrane and destroy the protein and DNA [145].

3.4. Iron oxide nanoparticles for drug delivery applications

Taking the unique advantages associated with the targeted DDSs such as efficient drug solubility and stability, accurate dosage and drug release controllability, and effective delivery of therapeutics to specific sites with low toxicity and side effects, allowed DDSs to be widely involved in the remediation of a broad spectrum of therapeutic agents [154]. Among them, magnetic nanoparticles (MNPs), particularly IONs were the most skyrocketing, scaled up DDSs owing to their various advantages such as facile fabrication and surface functionalization, biocompatibility, low toxicity, and biodegradability [155,156]. Moreover, the fabulous superparamagnetic responsiveness of IONs DDSs (drug delivery system) endows them with extra proficiency over the other DDSs, represented by the diagnostic (i.e. used as contrast agents for magnetic resonance imaging) and therapeutic capabilities (i.e.

hyperthermia, magnetic targeting, and drug delivery) [157]. In addition to being superparamagnetic, IONPs, in either the magnetite (Fe₃O₄) or the maghemite (Fe₂O₃) form, have low toxicity and high biocompatibility, two features that have been attributed to the well-regulated endogenous mechanisms for iron homeostasis in humans [158,159]. Furthermore, IONs do not cause oxidative stress, even at high doses, and are effectively cleared from the body as a result of their biodegradability [158,159]. Owing to these excellent merits, IONs have displayed their potentiality for translation from bench to clinic. Notably, with a flexible surface chemistry of IONs, many drugs and bioactive molecules can be loaded onto the surface, forming drug-conjugated IONs system [160]. Based on the therapeutic application, drug molecules can be efficiently loaded with different surface functionalization strategies such as covalent conjugation (chemical surface modification) [161], and non-covalent conjugation (encapsulation or adsorption) [162]. In this context, this section will discuss the different types of surface drug conjugation strategies for IONs targeted delivery systems, depicting their advantages, limitations, and challenges.

3.4.1. Non-covalent drug-conjugated iron oxide nanoparticles

In general, non-covalent conjugation involves physical interactions between the drug molecules and the surface of the nanoparticles without any modification of the chemical structure or the therapeutic activity of the molecule. Such approach is considered the most cost-effective, and simplest drug loading strategy because it does not require any chemical reagent or drastic fabrication conditions, thus lowering the toxicity of the drug molecules, and so providing a promising prototype for scalable and biocompatible DDSs for the clinical applications.

It is noteworthy that coating magnetic nanoparticles with porous materials such as silica was considered an innovative strategy for encapsulation of many stimuli sensitive drugs as well as controlling the release of the nanocarriers. In this context, the anticancer potentiality of HPC-grafted to silica coated magnetic nanoparticles encapsulated with a thermosensitive GEM (Gemcitabine) was investigated against pancreatic cancer cells through applying chemohyperthermia [163]. Remarkably, GEM loaded MNPs achieved a dramatic decrease in the cell growth from 60 to 20 and 12% after raising the temperature from 42 to 45 °C for 30 min, respectively indicating the outstanding synergy between the intra-tumoral injection of GEM and the induced magnetic heating treatment for the cancer cells. Moreover, the *in vivo* investigations with a viable MRI (magnetic resonance imaging) of tumor delivery confirmed the efficiency of the chemohyperthermia, showing an increased apoptotic cells death of 38%, outperforming the hyperthermia (14.7%) and chemotherapy (17.5%). Another noteworthy study done by Lee et al. demonstrated the theranostic applicability of core-shell iron oxide NPs coated with silica and functionalized with glutathione sensitive gatekeeper cyclodextrin (Fe@Si-DOX-CD-PEG) for the efficient encapsulation and controlled release of anticancer DOX [164]. Owing to the high concentration of GSH in the cytoplasmic tumor cells compared with the extracellular environment, Fe@Si-DOX-CD-PEG accomplished excellent *in vivo* drug release and cytotoxicity to A549 cells (human lung carcinoma) without premature release of DOX in the blood stream. This controlled and selective release achieved by Fe@Si-DOX-CD-PEG was attributed to the cleavage of disulfide stalk unit of CD gatekeeper that tightly bonded to the silica, thus enabling the rapid release of the entrapped drug molecules under suitable conditions. For sure, *in vivo* MRI exhibited a remarkable tumor growth inhibition for 7-9 days after the intravenous injection of Fe@Si-DOX-CD-PEG, establishing its proficiency as a platform for anticancer agents.

3.4.2. Covalent drug-conjugated iron oxide nanoparticles

In order to accomplish efficient covalent loading of drug molecules into IONs, several things must be taken into account such as the biocompatibility and biodegradability of the covalent linkage. This is in addition to the biological environment that directly influences the activity of the covalent linkage, in turns tuning the release profile of the

Table 2
Shows the MIC of iron oxides for diverse organisms.

Materials	Sensible organisms	MIC (mg/mL)	Refs.
SiO ₂ -Fe ₂ O ₃	<i>Candida parapsilosis</i> (<i>C. parapsilosis</i>)	0.31	[137]
	<i>Aspergillus niger</i> (<i>A. niger</i>)	0.21	
Fe ₂ O ₃ -ZrO ₂ /BC	<i>Escherichia coli</i> (<i>E. coli</i>)	0.030	[141]
GO/Ag/Fe ₂ O ₃	<i>E. coli</i>	0.043	[146]
	<i>Bacillus subtilis</i> (<i>B. subtilis</i>)	0.086	
FeO	<i>E. coli</i>	2.5	[147]
	<i>Staphylococcus Aureus</i> (<i>S. aureu</i>)	5.0	
CT-Fe ₃ O ₄	<i>S. aureus</i>	0.5	[148]
JC-Fe ₃ O ₄	water-borne	1	
CT-Fe ₃ O ₄		0.25	
JC-Fe ₃ O ₄		0.5	
GO/Fe ₃ O ₄ /NPVP/	<i>E. coli</i>	0.031	[149]
Ag	<i>S. aureus</i>	0.062	
Iron oxide nanorodes	<i>Pseudomonas aeruginosa</i> (<i>P. aeruginosa</i>)	0.510	[150]
Fe ₂ O ₃ nanoparticles	(<i>Trichothecium roseum</i>) <i>T. roseum</i>	0.063	[151]
	(<i>Cladosporium herbarum</i>) <i>C. herbarum</i>	0.063	
	(<i>Penicillium chrysogenum</i>) <i>P. chrysogenum</i>	0.016	
	<i>A. alternata</i>	0.032	
	<i>A. niger</i>	0.016	
DIONPs	(<i>Staphylococcus epidermidis</i>) <i>S. epidermidis</i>	0.016	[152]
	<i>E. coli</i>		
IONPs	<i>S. aureus</i>	0.013	[153]
	<i>E. coli</i>	0.012	
	<i>Shigella dysenteriae</i> (<i>S. dysenter</i>)	0.012	

nano-vehicles. Thus, the change in the chemical structure and orientation of the drug molecules after the covalent conjugation with the nanoparticles may affect their biological activity [165]. However, the insufficient loading efficiency of the drug molecules, the drug release difficulty, and the utilization of chemical and catalytic reagent for the covalent bond formation that may cause *in vivo* cytotoxicity limit the efficacy of such approach in practice. Based on the bond motifs, the covalent conjugation of the drug molecules with IONs is classified into three common types of covalent attachment including amide linkages [166], pH-degradable (i.e., acid cleavable) [167], and enzymatically cleavable bonds (Table 3) [168].

Acid cleavable bonds (pH sensitive DDSs) are the most commonly used covalent drug-NPs conjugation system [169]. Due to the ease of fabrication and high pH sensitivity of hydrazone bond conjugation, such approach has been widely *in vitro* and *in vivo* investigated [170]. For instance, a pH-sensitive DOX hydrazone linked PMMA coated magnetic FeO nanocubes (N-PMNC@DOX) was *in vitro* and *in vivo* tested against tumor cells of Hela cells and tumor-bearing mice (Fig. 5 (A-B)) [171]. N-PMNC@DOX exhibited high drug release (84%) at pH = 5 (i.e. similar to endosomes and lysosomes of cancer cells) compared with pH = 7.4 (i.e. physiological pH) after 40 h. Such result indicated the sensitivity of hydrazone bond at acidic medium mimic to the cancer cells, thus achieving a controlled release and targeted delivery to the tumor cells. Therefore, cell counting assay kit-8 (CCK-8) confirmed the cytotoxicity of N-PMNC@DOX against Hela cells, showing a great proliferative inhibition of Hela cells growth after 6, 12, 24 h due to the efficient internalization and cellular uptake of N-PMNCs associated with the hydrophilicity of hydrazide, and so the excellent dispersion in cell medium. Importantly, *in vivo* analysis confirmed the outstanding anticancer efficacy of N-PMNC@DOX against nude mice bearing Hela (cervical cancer cell line) tumor, showing a remarkable tumor growth inhibition after employing an external magnetic field for efficient targeted delivery

with negligible side effects. Another example displayed a synergistic theranostics for tumor cells using cystamine *tert*-acylhydrazine attached to PEG coated superparamagnetic iron oxide covalently loaded with DOX via acylhydrazone bond ($\text{Fe}_3\text{O}_4/\text{CTA}/\text{DOX}/\text{PEG}$) (Fig. 5C) [172]. $\text{Fe}_3\text{O}_4/\text{CTA}/\text{DOX}/\text{PEG}$ displayed a sustained release of DOX under acidic conditions due to the cleavage of pH-sensitive acylhydrazone bond, showing an excellent *in vivo* growth inhibition of tumor bearing mice with a simultaneous MRI. In contrast, Wang et al. demonstrated a rapid release of DOX for the simultaneous chemotherapy and diagnosis of hepatocellular carcinoma cells using DOX loaded targeting peptide (SP94) covalently conjugated to amine functionalized Fe_3O_4 through acidic sensitive hydrazone bond comparable to the previous example [170]. These results unveiled that there are other parameters that affect the release of the covalently conjugated drug molecules rather than the pH sensitivity such as the synthetic route of the hydrazone bond and the hydrophilicity of the surface of IONs that immensely affect the release attitude, and the efficiency of internalization and cellular uptake of the nanoparticles. Further, Zhao and coworkers exhibited a noticeable *in vitro* cytotoxicity of arginine-glycine-aspartic acid modified magnetic nanoparticle conjugated with DOX via acid labile imine bond (Schiff base) against both U-87 MG glioblastoma brain cells ($\text{IC}_{50} = 0.93 \mu\text{g/mL}$ in 24h) and MCF7 breast cells ($\text{IC}_{50} = 0.06 \mu\text{g/mL}$ in 24h) comparable to free DOX [171]. This finding was mainly associated with the good cellular uptake of the nanoparticles *via* endocytosis and the acidic pH sensitivity of the imine bond inside the cancer cells (endosomes and lysosomes). In addition, the magnetic nanocarrires achieved a superior cytotoxicity under external magnetic field due to the increased concentration of the drug carrier around the cancer cells.

Considering the thermal stability, resistance to degradation by cellular protease and hydrolysis at low pH, covalent drug conjugation with IONs *via* amide bond reinforces its thermal stability, and provide a sustained release profile with long lifetime of the drug carrier in the

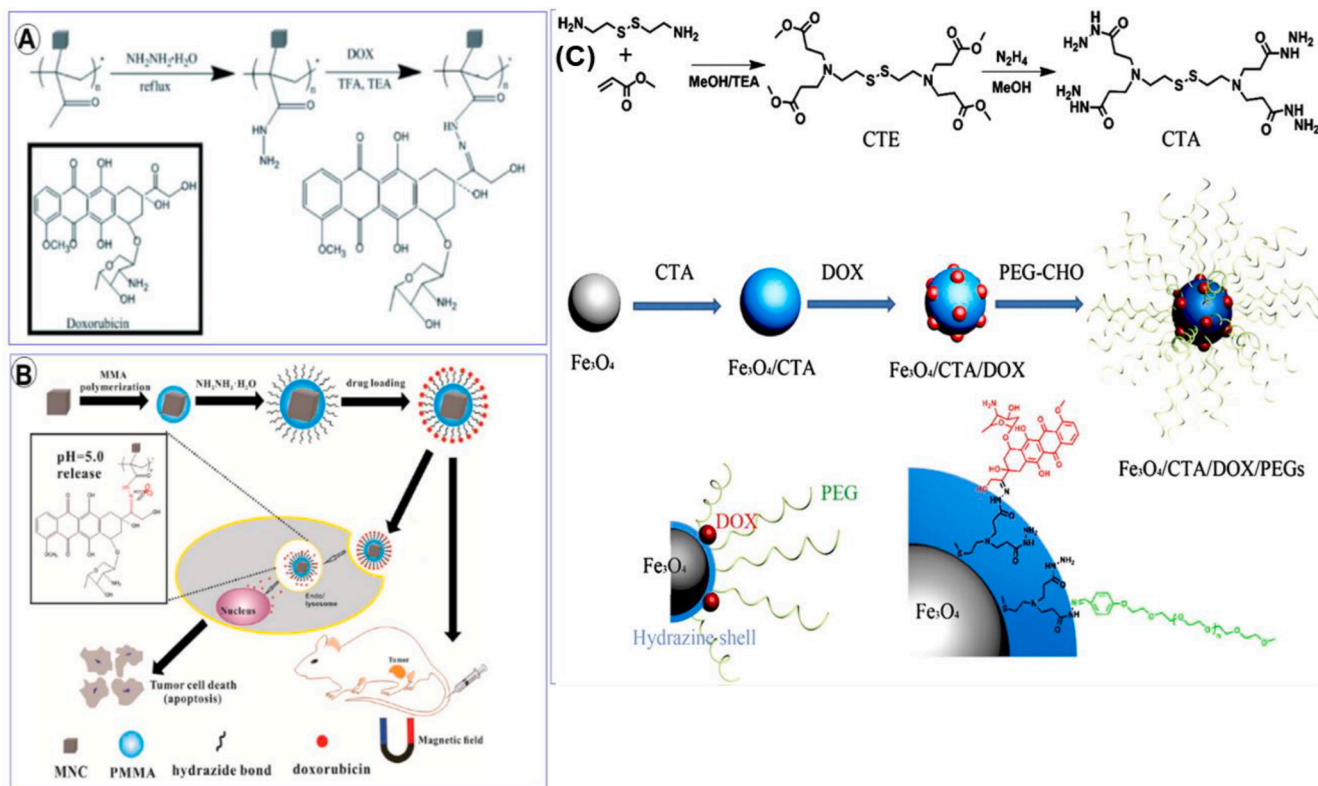


Fig. 5. (A) Synthetic route of pH-responsive N-PMNCs@DOX. TFA = trifluoroaceticacid, TEA = triethylamine; and (B) Schematic illustration of the fabrication of an intracellular pH-responsive drug delivery system based on MNCs for remotely targeted tumor therapy *in vitro* and *in vivo*. Reproduced with permission [171] Copyright 2014, American Chemical Society, (C) The preparation route of the $\text{Fe}_3\text{O}_4/\text{CTA}/\text{DOX}/\text{PEG}$ nanocomposites, Reproduced with permission [172] Copyright 2013, Elsevier.

blood circulation. In this line, Hua et al. developed a water soluble thermally stable magnetic targeted drug carrier constituted of hydrophobic paclitaxel drug (PTX) conjugated through amide bond with poly [aniline-co-sodium N-(1-one-butryic acid) aniline] doped with HCl aqueous solution (SPAnH) modified MNPs (shell/core) (PAh/MNPs-bound-PTX) for the chemotherapy of human prostate cells [172]. XTT assay demonstrated an *in vitro* reduced cell viability of PC3 ($IC_{50} = 9.7 \mu\text{g}/\text{mL}$) and CWR22R cells (human prostate cancer cell line) ($IC_{50} = 4.2 \mu\text{g}/\text{mL}$) after incubation with PAh/MNPs-bound-PTX for 8h comparable to free PTX ($IC_{50} = 11.1 \mu\text{g}/\text{mL}$) and ($IC_{50} = 7.1 \mu\text{g}/\text{mL}$), respectively. Such result was related to the efficient and rapid cellular uptake of PAh/MNPs *via* clathrin and caveolae endocytosis, and the improved water solubility of PTX. Moreover, PAh/MNPs-bound-PTX accomplished a higher cytotoxicity after employing a magnetic targeting delivery against PC3 ($IC_{50} = 4.6 \mu\text{g}/\text{mL}$) and CWR22R ($IC_{50} = 1.7 \mu\text{g}/\text{mL}$) cells, establishing a promising therapeutic efficacy with minimal injection dosage and side effects. Another innovative therapeutic strategy was proposed by Yang et al. for the effective chemotherapy of prostate cancer, involving dual functionalization of magnetic nanoparticles with carboxylated *o*-(2-aminoethyl) polyethylene glycol ($\text{NH}_2\text{-EPEG-COOH}$) and antiprostate-specific membrane antigen antibodies to enhance the uptake of the nanoparticles by reticuloendothelial system and the binding efficacy to the cellular membrane of the prostate cancer cells [173]. Owing to the binding efficiency of PTX-HMNC-EPEG-APSMA (64.8%) to the cellular membrane, and the excellent internalization of the nanoparticles into CWR22R mouse xenograft *via* different endocytic mechanisms (caveolae-mediated endocytosis, macropinocytosis, or clathrin-mediated endocytosis), the concentration of the target delivered PTX was increased by 20-fold comparable to free PTX injection. Accordingly, PTX-HMNC-EPEG-APSMA achieved an efficient tumor growth inhibition with prolonged survival period of the tumor bearing mice from 35 to 58 days with smaller loaded dose of PTX (4.5 mg/kg) than free PTX (6 mg/kg). Hence, these outstanding results indicated the *in vivo* potential applicability of PTX-HMNC-EPEG-APSMA against human prostate cells.

Recently, Ansari et al. suggested a novel anticancer therapeutic strategy, combining the *in vivo* MR imaging of the targeted delivery and the tumor location, and the chemotherapy using cross linked IONPs conjugated with azademethylcolchicine *via* MMP-14 cleavable peptide linker (AlaCysArgSerCitGly-HPheTyrLeuTyr) (CLIO-ICT) (Fig. 6 a) (Table 3) [174]. Azademethylcolchicine is a vascular disrupting agent (VDS) that indirectly suppresses tumors growth through the destabilization of the endothelium resulting in an increase in the vascular permeability and collapse of intratumoral blood vessels, thus blocking the blood flow towards the tumor cell and enhancing the EPR effect (i.e. drug targeting and retention at the tumor site) [175,176]. Accordingly, CLIO-ICT exhibited an obvious cytotoxicity to breast cancer cells (MMTV-PyMT). This behavior was attributed to the conversion of CLIO-ICT from non-toxic to an active reagent *via* the selective cleavage of the peptide linker *via* MMP-14 enzyme, releasing azademethylcolchicine (VDS) (Fig. 6 b) that abolished the tumor proliferation through the long retention of the drug molecules in the tumor tissue without any side effect on the normal cells. In addition, the magnetic core provides a possibility for the *in vivo* MRI of the tumor localization and disease extent, offering an innovative and effective theranostics of the tumor cells. Further, Lee et al. asserted the anticancer activity of urokinase plasminogen activator receptor (uPAR) targeted IONPs conjugated with gemcitabine (Gem) *via* lysosomal (Cathepsin B) cleavable amine terminal peptide linker (ATF-IONP-Gem) against pancreatic cancer [177,178]. Notably, ATF-IONP-Gem exhibited 82% Gem release in presence of lysosomal enzyme at pH = 5.5 mimic to the endosomes or lysosomes of the intracellular vesicles of the pancreatic cancer cells compared with at pH = 7.4 (physiological environment) of 40% release. Thus, cell proliferation assay for MIA Paca-2 human pancreatic cells unveiled lower cell viability of 29% associated with ATF-IONP-Gem than free Gem and IONP-Gem. Therefore, ATF-IONP-Gem displayed a significant tumor growth inhibition for orthotopic human pancreatic cancer xenografts in nude mice of 50% higher than Gem (30%) and IONP-Gem (23%). Such a remarkable tumor growth inhibition was related to the efficient endocytic internalization of the nanoparticles

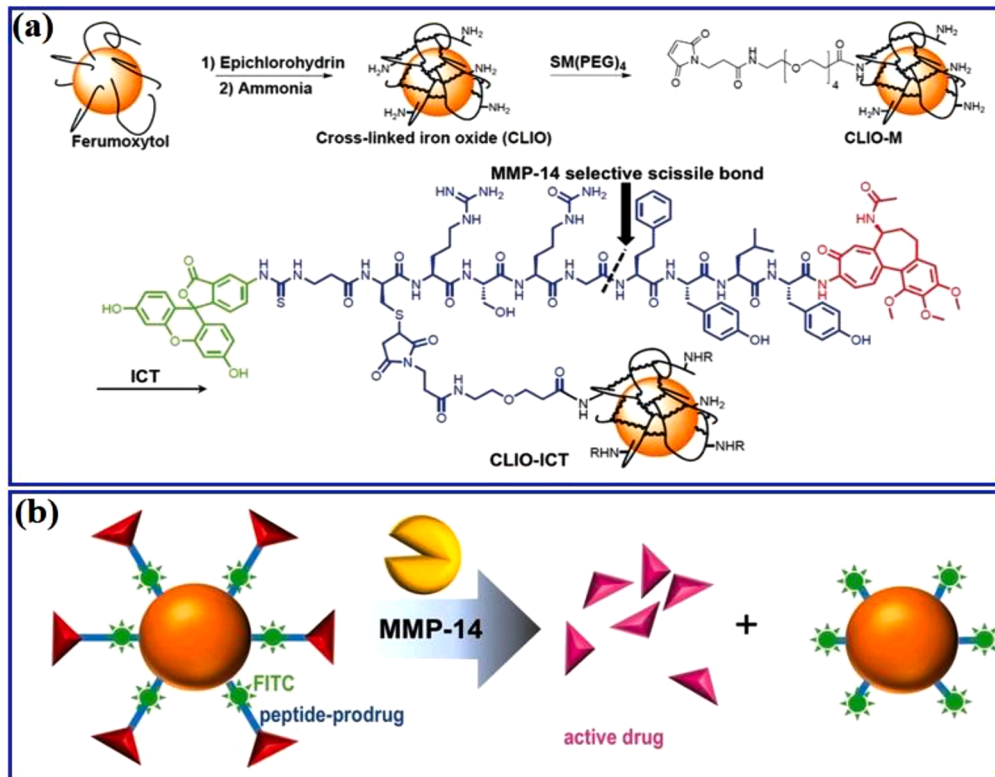


Fig. 6. (a) Schematic representation of theranostic nanoparticle (TNP) activation by MMP-14: the IONP core is shown in orange; the prodrug ICT is shown in red, and after MMP-14 activation, its product is shown in magenta; the peptide linker is shown in blue, and the FITC is shown in green. (b) Synthesis of the theranostic nanoparticles. FITC (shown in green) is linked to the TNP via the amino group of cysteine, Reproduced with permission [174]. Copyright 2014, Wiley. (For interpretation of the references to color in this figure legend, the reader is referred to the web version of this article.)

Table 3

Summary of some anticancer agents loaded into iron oxide nanocarriers by different conjugation routes.

Drug carrier	Drug loaded	Cell tested	Conjugation type	Refs.
DOX@Fl-PMNPs	Doxorubicin	Breast cancer cells, primary tumor cells, and solid tumors.	Non-covalent (adsorption/complexation)	[164]
DOX loaded PEGylated SPIONs	Doxorubicin	MDA-MB435 cell / xenograft breast tumors in nude mice	Non-covalent (complexation)	[165]
MF66-N6L-Dox	Doxorubicin	MDA-MB-231 tumor bearing female athymic nude mice	Non-covalent (electrostatic attraction)	[166]
Gem-HPC-grafted porous magnetic drug carrier	Gemcitabine	pancreatic cancer cells	Non-covalent (encapsulation)	[167]
Fe@Si-DOX-CD-PEG	Doxorubicin	A549 cells (human lung carcinoma)	Non-covalent (encapsulation)	[168]
Cisplatin-loaded iron oxide nanoparticles	cisplatin (IV) prodrug	Ovarian cancer A2780 and A2780cis cells	Non-covalent (complexation)	[179]
Folate-PEOz-PLA/IOP/PTX mice	Paclitaxel	Hela cells and tumor-bearing		[180]
N-PMNC@DOX mice	Non-covalent (encapsulation)	[180]		
Doxorubicin	Covalent (Acid cleavable bond / hydrazone bond)	Hela cells and tumor-bearing		[171]
Fe ₃ O ₄ /CTA/DOX/PEG mice	Doxorubicin	[171]		
Covalent (Acid cleavable bond/ hydrazone bond)	Doxorubicin	Hela cells and tumor-bearing		[172]
Fe ₃ O ₄ -DOX/SP94 cell (HepG2)	Doxorubicin	[172]		
Covalent (Acid cleavable bond/ hydrazone bond)	Doxorubicin	Human hepatocellular carcinoma		[170]
DOX conjugated with arginine-glycine-ascorbic acid modified magnetic nanoparticle.	Doxorubicin	U-87 MG glioblastoma brain cells and MCF7 breast cells	Covalent (Acid cleavable bond/Imine bond)	[173]
PAnH/MNPs-bound-PTX (PC3 (prostate cancer cell line)and CWR22R)	Paclitaxel	Human prostate carcinoma cells		[174]
PTX-HMNC-EPEG-APSMA	Covalent (Amide bond)	[174]		
Paclitaxel	Paclitaxel	CWR22R mouse xenograft and human prostate cells	Covalent (Amide bond)	[175]
CLIO-ICT	Azademethylcolchicine	Breast cancer cells (MMTV-PyMT)	Covalent (Enzymatic cleavable bond)	[176]
ATF-IONP-Gem	Gemcitabine	Orthotopic human pancreatic cancer xenografts in nude mice	Covalent (Enzymatic cleavable bond)	[172]

into the cell that was simultaneously visualized by MRI, and then the selective cleavage of the tetrapeptide linker *via* Cathepsin B inside the cancerous cell to release the Gem anticancer agent to kill the tumor.

4. Conclusion and perspectives

In the present review, different synthesis approaches of iron oxide nanoparticle were briefly reviewed and highlighted. Furthermore, rich discussion regarding the exfoliation of various forms of iron oxide nanoparticles in pharmaceutical applications was reviewed. Moreover, good interpretation for the efficiency of iron oxide nanoparticles usage for drug delivery, anticancer, antiviral and antimicrobial applications was executed. Variety of reported systems based on IOPs were reviewed as anticancer agents against various cancer cells exploited in *in vitro* or *in vivo* studies. Moreover, detailed review was implemented about exploitation of different IOPs systems against different bacterial lines and virus. Additionally, the influence of iron oxide nanoparticle size and synthesis method conditions were also discussed. Finally, the suggested mechanistic actions of iron oxide nanoparticles toward each pharmaceutical application for boosting their efficacy were also reported. Accordingly, there are various obstacles facing the scientists regarding the design and synthesis of safe and efficient IOPs based systems for pharmaceutical applications. Therefore, to overcome these drawbacks intensive researches are required for design and development of green hybrid systems based tunable IOPs size own convenient physico-chemical and magnetic properties.

Declaration of Competing Interest

The authors declare that they have no known competing financial interests or personal relationships that could have appeared to influence the work reported in this paper.

References

- [1] A.G. Roca, L. Gutiérrez, H. Gavilán, M.E. Fortes Brollo, S. Veintemillas-Verdaguer, M. del Puerto Morales, Design strategies for shape-controlled magnetic iron oxide nanoparticles, *Adv. Drug Deliv. Rev.* 138 (2019) 68–104.
- [2] T. Trindade, P.J. Thomas, *Defining and Using Very Small Crystals, Volume 4*, Elsevier Ltd., Amsterdam, The Netherlands, 2013. ISBN 9780080965291.
- [3] M.C. Tringides, M. Jalochnowski, E. Bauer, Quantum size effects in metallic nanostructures, *Phys. Today* 60 (2007) 50–54.
- [4] Q. Li, C.W. Kartikowati, S. Horie, T. Ogi, T. Iwaki, K. Okuyama, Correlation between particle size/domain structure and magnetic properties of highly crystalline Fe₃O₄ nanoparticles, *Sci. Rep.* 7 (2017) 1–7.
- [5] Y. Sun, S.K. Gray, S. Peng, Surface chemistry: A non-negligible parameter in determining optical properties of small colloidal metal nanoparticles, *Phys. Chem. Chem. Phys.* 13 (2011) 11814–11826.
- [6] S. Fang, D. Bresser, S. Passerini, Transition metal oxide anodes for electrochemical energy storage in lithium- and sodium-ion batteries, *Adv. Energy Mater.* 10 (2020) 10.
- [7] T. Kostyantyn, Z. Turek, M. Zanáška, P. Kudrna, M. Tichý, Iron oxide and iron sulfide films prepared for dye-sensitized solar cells, *Materials* 13 (2020) 1797.
- [8] R.G.D. Andrade, S.R.S. Veloso, E.M.S. Castanheira, Shape anisotropic iron oxide-based magnetic nanoparticles: synthesis and biomedical applications, *Int. J. Mol. Sci.* 21 (2020) 2455.
- [9] V. Magdanz, J. Gebauer, P. Sharan, S. Eltoukhy, D. Voigt, J. Simmchen, Sperm–particle interactions and their prospects for charge mapping, *Adv. Biosyst.* 3 (2019) 1–23.
- [10] M. Rui, C. Ma, Y. Hao, J. Guo, Y. Rui, X. Tang, Q. Zhao, X. Fan, Z. Zhang, T. Hou, Iron oxide nanoparticles as a potential iron fertilizer for peanut (*Arachis hypogaea*), *Front. Plant Sci.* 7 (2016) 815.
- [11] N.F. Attia, J. Park, H. Oh, Facile tool for green synthesis of graphene sheets and their smart free-standing UV protective film, *Appl. Surf. Sci.* 458 (2018) 425–430.
- [12] S.E.A. Elashery, N.F. Attia, M.M. Omar, H.M.I. Tayea, Cost-effective and green synthesized electroactive nanocomposite for high selective potentiometric determination of clomipramine hydrochloride, *Microchem. J.* 151 (2019), 104222.
- [13] A.M. ElSawy, N.F. Attia, H.I. Mohamed, M. Mohsen, M.H. Talaat, Innovative coating based on graphene and their decorated nanoparticles for medical stent applications, *Mater. Sci. Eng. C* 96 (2019) 708–715.
- [14] N.F. Attia, H. Ahmed, D. Yehia, M. Hassan, Y. Zaddin, Novel synthesis of nanoparticles-based back coating flame-retardant materials for historic textile fabrics conservation, *J. Ind. Text.* 46 (2017) 1379–1392.
- [15] N.F. Attia, A.M. Eid, M.A. Soliman, M. Nagy, Exfoliation and decoration of graphene sheets with silver nanoparticles and their antibacterial properties, *J. Polym. Environ.* 26 (2018) 1072–1077.

- [16] N.F. Attia, M. Mousa, Synthesis of smart coating for furniture textile and their flammability and hydrophobic properties, *Prog. Org. Coat.* 110 (2017) 204–209.
- [17] N.F. Attia, K. Abdel Hady, S.E.A. Elashery, H.M. Hashem, H. Oh, A.M. Refaat, A. Abdel Hady, Greener synthesis route and characterization of smart hybrid graphene based thin films, *Surf. Interfaces* 21 (2020), 100681.
- [18] M. Jung, J. Park, S.Y. Cho, S.E.A. Elashery, N.F. Attia, H. Oh, Flexible carbon sieve based on nanoporous carbon cloth for efficient CO₂/CH₄ separation, *Surf. Interfaces* 23 (2021), 100960.
- [19] N.F. Attia, S.E.A. Elashery, A.M. Zakria, A.S. Eltaweil, H. Oh, Recent advances in graphene sheets as new generation of flame retardant materials, *Mater. Sci. Eng.* 274 (2021), 115460.
- [20] A.S. Eltaweil, A.M. Omer, H.G. El-Aqapa, N.M. Gaber, N.F. Attia, G.M. El-Subrui, M.S. Mohy-Eldin, M. E, Abd El-Monaem, Chitosan based adsorbents for the removal of phosphate and nitrate: a critical review, *Carbohydr. Polym.* 274 (2021), 118671.
- [21] M. Yusefi, K. Shamel, R.R. Ali, S.W. Pang, S.Y. Teow, Evaluating anticancer activity of plant-mediated synthesized iron oxide nanoparticles using Punica granatum fruit peel extract, *J. Mol. Struct.* 1204 (2020), 127539.
- [22] N.S. Sallabani, S. Singh, Recent advances and future prospects of iron oxide nanoparticles in biomedicine and diagnostics, *Biotech* 8 (2018) 1–23.
- [23] Z. Chen, C. Wu, Z. Zhang, W. Wu, X. Wang, Z. Yu, Synthesis, functionalization, and nanomedical applications of functional magnetic nanoparticles, *Chin. Chem. Lett.* 29 (2018) 1601–1608.
- [24] S.A.M.K. Ansari, E. Ficiarà, F.A. Ruffinatti, I. Stura, M. Argenziano, O. Abollino, F. D'Agata, Magnetic iron oxide nanoparticles: synthesis, characterization and functionalization for biomedical applications in the central nervous system, *Materials* 12 (2019) 465.
- [25] A. Radóń, A. Drygala, L. Hawelek, D. Łukowiec, Structure and optical properties of Fe3O4 nanoparticles synthesized by co-precipitation method with different organic modifiers, *Mater. Charact.* 131 (2017) 148–156.
- [26] S.M. Dadfar, K. Roemhild, N.L. Drude, S. von Stillfried, R. Knüchel, F. Kiessling, T. Lammers, Iron oxide nanoparticles: diagnostic, therapeutic and theranostic applications, *Adv. Drug Deliv. Rev.* 138 (2019) 302–325.
- [27] L.S. Arias, J.P. Pessan, A.P.M. Vieira, T.M.T.D. Lima, A.C.B. Delbem, D. R. Monteiro, Iron oxide nanoparticles for biomedical applications: a perspective on synthesis, drugs, antimicrobial activity, and toxicity, *Antibiotics* 7 (2018) 46.
- [28] A.V. Samrot, C.S. Sahithya, J. Selvarani, S.K. Purayil, P. Ponnaiah, A review on synthesis, characterization and potential biological applications of superparamagnetic iron oxide nanoparticles, *Curr. Res. Green Sustain. Chem.* 4 (2019), 100042.
- [29] S. Hasany, H. Abdurahman, A. Sunarti, R. Jose, Magnetic iron oxide nanoparticles: chemical synthesis and applications review, *Curr. Nanosci.* 9 (2013) 561–575.
- [30] M. Parashar, V.K. Shukla, R. Singh, Metal oxides nanoparticles via sol-gel method: a review on synthesis, characterization and applications, *J. Mater. Sci.* 31 (2020) 3729–3749.
- [31] Z.N. Kayani, S. Arshad, S. Riaz, S. Naseem, Synthesis of iron oxide nanoparticles by sol-gel technique and their characterization, *IEEE Trans. Magn.* 50 (2014) 1–4.
- [32] M. Yusefi, K. Shamel, A.F. Jumaat, Preparation and properties of magnetic iron oxide nanoparticles for biomedical applications: a brief review, *J. Adv. Res. Mater. Sci.* 75 (2020) 10–18.
- [33] A. Hassanjani-Roshan, M.R. Vaezi, A. Shokuhfar, Z. Rajabali, Synthesis of iron oxide nanoparticles via sonochemical method and their characterization, *Paticulology* 9 (2011) 95–99.
- [34] M.N. Islam, J.R. Jeong, C. Kim, A facile route to sonochemical synthesis of magnetic iron oxide (Fe₃O₄) nanoparticles, *Thin Solid Films* 519 (2011) 8277–8279.
- [35] N. Shin, K. Saravanakumar, M.H. Wang, Sonochemical mediated synthesis of iron oxide (Fe₃O₄ and Fe₂O₃) nanoparticles and their characterization, cytotoxicity and antibacterial properties, *J. Clust. Sci.* 30 (2019) 669–675.
- [36] A.V. Nikam, B.L.V. Prasad, A.A. Kulkarni, Wet chemical synthesis of metal oxide nanoparticles: a review, *Cryst. Eng. Comm.* 20 (2018) 5091–5107.
- [37] N.J. Orsini, B. Babić-Stojčić, V. Spasojević, M.P. Calatayud, N. Cvjetićanin, G. F. Goya, Magnetic and power absorption measurements on iron oxide nanoparticles synthesized by thermal decomposition of Fe (acac)₃, *J. Magn. Magn. Mater.* 449 (2018) 286–296.
- [38] G. Cotin, C. Kiefer, F. Perton, D. Ihiawakrim, C. Blanco-Andujar, S. Moldovan, S. Bégin-Colin, Unravelling the thermal decomposition parameters for the synthesis of anisotropic iron oxide nanoparticles, *Nanomaterials* 8 (2018) 881.
- [39] S. Dixit, P. Jeevanandam, Synthesis of iron oxide nanoparticles by thermal decomposition approach, *Advanced Materials Research* 67, Trans Tech Publications Ltd, 2009, pp. 221–226.
- [40] J.A. Siddique, N.F. Attia, K.E. Geckeler, Polymer nanoparticles as a tool for the exfoliation of graphene sheets, *Mater. Lett.* 158 (2015) 186–189.
- [41] A. Scano, V. Cabras, M. Pilloni, G. Ennas, Microemulsions: the Renaissance of ferrite nanoparticle synthesis, *J. Nanosci. Nanotechnol.* 19 (2019) 4824–4838.
- [42] O.A. Noqta, A.A. Aziz, I.A. Usman, M. Bououdina, Recent advances in iron oxide nanoparticles (IONPs): synthesis and surface modification for biomedical applications, *J. Supercond. Novel Magn.* 32 (2019) 779–795.
- [43] C. Okoli, M. Sanchez-Dominguez, M. Boutonnet, S. Jaras, C. Civera, C. Solans, G. R. Kuttuva, Comparison and functionalization study of microemulsion-prepared magnetic iron oxide nanoparticles, *Langmuir* 28 (2012) 8479–8485.
- [44] A. Lassoued, M.S. Lassoued, B. Dkhil, S. Ammar, A. Gadri, Synthesis, photoluminescence and Magnetic properties of iron oxide (α -Fe₂O₃) nanoparticles through precipitation or hydrothermal methods, *Phys. E* 101 (2018) 212–219.
- [45] P. Bhavani, C.H. Rajababu, M.D. Arif, I.V.S. Reddy, N.R. Reddy, Synthesis of high saturation magnetic iron oxide nanomaterials via low temperature hydrothermal method, *J. Magnet. Magnet. Mater.* 426 (2017) 459–466.
- [46] C. Song, W. Sun, Y. Xiao, X. Shi, Ultrasmall iron oxide nanoparticles: Synthesis, surface modification, assembly, and biomedical applications, *Drug Discov. Today* 24 (2019) 835–844.
- [47] J.A. Siddique, N.F. Attia, N. Tyagi, K.E. Geckeler, Exfoliated graphene sheets: polymer nanoparticles as a tool and their anti-proliferative activity, *ChemistrySelect* 4 (2019) 13204–13209.
- [48] C. Iacovita, I. Fizeşan, A. Pop, L. Scorus, R. Dudric, G. Stiuflciu, C. Lucaci, In vitro intracellular hyperthermia of iron oxide magnetic nanoparticles, synthesized at high temperature by a polyol process, *Pharmaceutics* 12 (2020) 424.
- [49] S.F. Hasany, I. Ahmed, J. Rajan, A. Rehman, Systematic review of the preparation techniques of iron oxide magnetic nanoparticles, *Nanosci. Nanotechnol* 2 (2012) 148–158.
- [50] J. Wallyn, N. Anton, T.F. Vandamme, Synthesis, principles, and properties of magnetite nanoparticles for in vivo imaging applications-A review, *Pharmaceutics* 11 (2019) 601.
- [51] A. Ali, M.Z. Hira Zafar, I. ul Haq, A.R. Phull, J.S. Ali, A. Hussain, Synthesis, characterization, applications, and challenges of iron oxide nanoparticles, *Nanotechnol. Sci. Applat.* 9 (2016) 49.
- [52] R. Hachani, M. Lowdell, M. Birchall, A. Hervault, D. Mertz, S. Begin-Colin, N.T. K. Thanh, Polyol synthesis, functionalisation, and biocompatibility studies of superparamagnetic iron oxide nanoparticles as potential MRI contrast agents, *Nanoscale* 8 (2016) 3278–3287.
- [53] A. Erwin, S. Salomo, P. Adhy, N. Utari, W. Ayu, Y. Wita, S. Nani, Magnetic iron oxide particles (Fe₃O₄) fabricated by ball milling for improving the environmental quality, in: IOP Conference Series: Materials Science and Engineering 845, 2020, 012051.
- [54] Y. Darvina, N. Yulfriska, H. Rifai, L. Dwiridal, R. Ramli, Synthesis of magnetite nanoparticles from iron sand by ball-milling, *J. Phys.* 1185 (2019), 012017.
- [55] J.F. De Carvalho, S.N. De Medeiros, M.A. Morales, A.L. Dantas, A.S. Carriço, Synthesis of magnetite nanoparticles by high energy ball milling, *Appl. Surf. Sci.* 275 (2013) 84–87.
- [56] R. Arbain, M. Othman, S. Palaniandy, Preparation of iron oxide nanoparticles by mechanical milling, *Miner. Eng.* 24 (2011) 1–9.
- [57] P.G. Jamkhande, N.W. Ghule, A.H. Bamer, M.G. Kalaskar, Metal nanoparticles synthesis: An overview on methods of preparation, advantages and disadvantages, and applications, *J. Drug Deliv. Sci. Technol.* 53 (2019), 101174.
- [58] A.V. Samrot, C.S. Sahithya, J. Selvarani, S.K. Purayil, P. Ponnaiah, A review on synthesis, characterization and potential biological applications of superparamagnetic iron oxide nanoparticles, *Cur. Res. Green Sust. Chem.* 4 (2021), 100042.
- [59] E. Fazio, M. Santoro, G. Lentini, D. Franco, S.P.P. Guglielmino, F. Neri, Iron oxide nanoparticles prepared by laser ablation: Synthesis, structural properties and antimicrobial activity, *Colloids Surf. A* 490 (2016) 98–103.
- [60] R.A. Ismail, G.M. Sulaiman, S.A. Abdulrahman, T.R. Marzoog, Antibacterial activity of magnetic iron oxide nanoparticles synthesized by laser ablation in liquid, *Mater. Sci. Eng.: C* 53 (2015) 286–297.
- [61] V.A. Svetlichnyi, A.V. Shabalina, I.N. Lapin, D.A. Goncharova, D.A. Velikanov, A. E. Sokolov, Study of iron oxide magnetic nanoparticles obtained via pulsed laser ablation of iron in air, *Appl. Surf. Sci.* 462 (2018) 226–236.
- [62] S. Kanagububalkshmi, K. Kadirvelu, Green synthesis of iron oxide nanoparticles using *Lagenaria siceraria* and evaluation of its antimicrobial activity, *Def. Life Sci. J.* 2 (2017) 422–427.
- [63] M. Khatami, H.Q. Alijani, B. Fakheri, M.M. Mobasser, M. Heydarpour, Z. K. Farahani, A.U. Khan, Super-paramagnetic iron oxide nanoparticles (SPIONs): Greener synthesis using Stevia plant and evaluation of its antioxidant properties, *J. Cleaner Prod.* 208 (2019) 1171–1177.
- [64] N. Beheshtkoo, M.A.J. Koubbanani, A. Savardshtaki, A.M. Amani, S. Taghizadeh, Green synthesis of iron oxide nanoparticles by aqueous leaf extract of *Daphne mezereum* as a novel dye removing material, *Appl. Phys. A* 124 (2018) 1–7.
- [65] A. M.Omer, R. Dey, A.S. Eltaweil, E.M. Abd El-Monaem, Z.M. Ziora, Insights into recent advances of chitosan-based adsorbents for sustainable removal of heavy metals and anions, *Arab. J. Chem.* 15 (2022), 103543.
- [66] E. El Bestawy, B.F. El-Shatby, A.S. Eltaweil, Integration between bacterial consortium and magnetite (Fe₃O₄) nanoparticles for the treatment of oily industrial wastewater, *World J. Micro. Biotechnol.* 36 (2020) 141.
- [67] S.A. Sallam, G.M. El-Subrui, A.S. Eltaweil, Facile synthesis of Ag- γ -Fe₂O₃ superior nanocomposite for catalytic reduction of methyl orange, *Catal. Lett.* 148 (2018) 3701–3714.
- [68] M.E.B. Mohamed, N.F. Attia, S.E.A. Elashery, Greener and facile synthesis of hybrid nanocomposite for ultrasensitive iron (II) detection using carbon sensor, *Micro. Meso. Mater.* 313 (2021), 110832.
- [69] E.Y. Frag, N.A. El-Zaher, S.E.A. Elashery, carbon thick sheet potentiometric sensor for selective determination of silver ions in X-ray photographic film, *Microchem. J.* 155 (2020), 104750.
- [70] S.E.A. Elashery, N.F. Attia, H. Oh, Design and fabrication of novel flexible sensor based on 2D Ni-MOF nanosheets as a preliminary step toward wearable sensor for onsite Ni (II) ions detection in biological and environmental samples, *Analy. Chim. Acta* 1197 (2022), 339518.
- [71] T.E. Elmetwally, S.S. Darwish, N.F. Attia, R.R.A. Hassan, A.A. El Ebisy, A. S. Eltaweil, A.M. Omer, H.R. El-Seedi, S.E.A. Elashery, Cellulose nanocrystals and

- its hybrid composite with inorganic nanotubes as green tool for historical paper conservation, *Prog. Org. Coat.* 168 (2022), 106890.
- [72] N. F.Attia, K.E. Geckeler, Polyaniline-polypyrrole composites with enhanced hydrogen storage capacities, *Macromol. Rapid Commun.* 34 (2013) 931–937.
- [73] J. Park, S.Y. Cho, M. Jung, K. Lee, Y.-C. Nah, N.F. Attia, H. Oh, Efficient synthetic approach for nanoporous adsorbents capable of pre-and post-combustion CO₂ capture and selective gas separation, *J. CO₂ Util.* 45 (2021) 101404.
- [74] N.F. Attia, M. Jung, J. Park, H. Jang, K. Lee, H. Oh, Flexible nanoporous activated carbon cloth for achieving high H₂, CH₄, and CO₂ storage capacities and selective CO₂/CH₄ separation, *Chem. Eng. J.* 379 (2020) 122367.
- [75] N.F. Attia, S.M. Lee, H.J. Kim, K.E. Geckeler, Nanoporous carbon-templated silica nanoparticles: Preparation, effect of different carbon precursors, and their hydrogen storage adsorption, *Micro. Meso. Mater.* 173 (2013) 139–146.
- [76] M. Jung, J. Park, K. Lee, N.F. Attia, H. Oh, Effective synthesis route of renewable nanoporous carbon adsorbent for high energy gas storage and CO₂/N₂ selectivity, *Renew. Energy* 161 (2020) 30–42.
- [77] A. Galal, M.M. Zaki, N.F. Attia, S.H. Samaha, H.E. Nasr, N.F. Attia, Electroremoval of copper ions from aqueous solutions using chemically synthesized polypyrrole on polyester fabrics, *J. Water Proc. Eng.* 43 (2021), 102287.
- [78] M.A. Diab, N.F. Attia, A.S. Attia, M.F. El-Shahat, Green synthesis of cost-effective and efficient nanoadsorbents based on zero- and two-dimensional nanomaterials for Zn²⁺ and Cr³⁺ removal from aqueous solutions, *Synth. Met.* 265 (2020), 116411.
- [79] N.F. Attia, S.M. Lee, H.J. Kim, K.E. Geckeler, Preparation of polypyrrole nanoparticles and their composites: effect of electronic properties on the hydrogen adsorption, *Polym. Int.* 64 (2015) 696–703.
- [80] N.F. Attia, M. Jung, J. Park, S.Y. Cho, H. Oh, Facile synthesis of hybrid porous composites and its porous carbon for enhanced H₂ and CH₄ storage, *Int. J. Hydrogen Energy* 45 (2020) 32797–32807.
- [81] N.F. Attia, Organic nanoparticles as promising flame-retardant materials for thermoplastic polymers, *J. Therm. Anal. Calorim.* 127 (2017) 2273–2282.
- [82] N.F. Attia, M.A. Diab, A.S. Attia, M.F. El-Shahat, Greener approach for fabrication of antibacterial graphene-polypyrrole nanoparticle adsorbent for removal of Mn²⁺ from aqueous solution, *Synth. Met.* 282 (2021), 116951.
- [83] S.R. Fouad, I.E. El-Sayed, N.F. Attia, M.M. Abdeen, A.H. Abdel Aleem, I.F. Nassar, H.I. Mira, E.A. Gawad, A. Kalam, A.A. Al-Ghamdi, A.A. Galhoun, Mechanistic study of Hg (II) interaction with three different α -aminophosphonate adsorbents: Insights from batch experiments and theoretical calculations, *Chemosphere* 304 (2022), 135253.
- [84] N.F. Attia, S.M. Shaltout, I.A. Salem, A.B. Zaki, M.H. El-Sadek, M.A. Salem, Sustainable and smart hybrid nanoporous adsorbent derived biomass as efficient adsorbent for cleaning of wastewater from Alizarin Red dye, *Biomass Conv. Bioref.* (2022), <https://doi.org/10.1007/s13399-022-02763-z>.
- [85] S. Kim, S.Y. Cho, K. Son, N.F. Attia, H. Oh, A metal-doped flexible porous carbon cloth for enhanced CO₂/CH₄ separation, *Sep. Purif. Technol.* 277 (2021), 119511.
- [86] N.F. Attia, H.E. Ahmed, A.A. El Ebissy, S.E.A. El Ashery, Green and novel approach for enhancing flame retardancy, UV protection and mechanical properties of fabrics utilized in historical textile fabrics conservation, *Prog. Org. Coat.* 166 (2022), 106822.
- [87] S.E.A. Elashery, N.F. Attia, G.G. Mohamed, M.M. Omar, H.M.I. Tayea, Hybrid nanocomposite based graphene sensor for ultrasensitive clomipramine HCl detection, *Electroanalysis* 33 (2021) 2361–2371.
- [88] W.G. El-Sayed, N.F. Attia, I. Ismail, M. El-Khayat, M. Nogami, M.S.A. Abdel-Mottaleb, Innovative and cost-effective nanodiamond based molten salt nanocomposite as efficient heat transfer fluid and thermal energy storage media, *Renew. Energy* 177 (2021) 596–602.
- [89] S.M. Mousavi, S.A. Hashemi, A. Gholami, N. Omidifar, M. Zarei, S. Bahrani, K. Yousefi, W.-H. Chiang, A. Babapoor, Bioinorganic synthesis of polyrhodanine stabilized Fe₃O₄/Graphene oxide in microbial supernatant media for anticancer and antibacterial applications, *Bioinorg. Chem. Applicat.* (2021), 2021.
- [90] H. Markides, M. Rotherham, A. El Haj, Biocompatibility and toxicity of magnetic nanoparticles in regenerative medicine, *J. Nanomater.* (2012), 2012.
- [91] A. Gholami, S. Rasoul-amini, A. Ebrahimezhad, S.H. Seradj, Y. Ghasemi, Lipoamino acid coated superparamagnetic iron oxide nanoparticles concentration and time dependently enhanced growth of human hepatocarcinoma cell line (Hep-G2), *J. Nanomater.* (2015), 451405, 2015.
- [92] E. Zachanowicz, J. Pigiowski, A. Zięcina, K. Rogacki, B. Poźniak, M. Tikhomirov, M. Maredziak, K. Marycz, J. Kisala, K. Hęclik, Polyrhodanine cobalt ferrite (PRHD@CoFe₂O₄) hybrid nanomaterials—Synthesis, structural, magnetic, cytotoxic and antibacterial properties, *Materi. Chem. Phys.* 217 (2018) 553–561.
- [93] M.B. Dastjerdi, A. Amini, M. Nazari, C. Cheng, V. Benson, A. Gholami, Y. Ghazemi, Novel versatile 3D bio-scaffold made of natural biocompatible hagfish exudate for tissue growth and organoid modeling, *Int. J. Biol. Macromol.* 158 (2020) 894–902.
- [94] T.K. Jana, S.K. Jana, A. Kumar, K. De, R. Maiti, A.K. Mandal, T. Chatterjee, B. K. Chatterjee, P. Chakrabarti, K. Chatterjee, The antibacterial and anticancer properties of zinc oxide coated iron oxide nanotextured composites, *Colloids Surf. B* 177 (2019) 512–519.
- [95] B. Malaikozhundan, B. Vaseeharan, S. Vijayakumar, K. Pandiselvi, M.A. R. Kalanjam, K. Murugan, G. Benelli, Biological therapeutics of Pongamia pinnata coated zinc oxide nanoparticles against clinically important pathogenic bacteria, fungi and MCF-7 breast cancer cells, *Micro. Pathog.* 104 (2017) 268–277.
- [96] M.A. Siddiqui, H.A. Alhadlaq, J. Ahmad, A.A. Al-Khedhairy, J. Musarrat, M. Ahamed, Copper oxide nanoparticles induced mitochondria mediated apoptosis in human hepatocarcinoma cells, *PloS One* 8 (2013) 69534.
- [97] Z. Izadiyan, K. Shameli, M. Miyake, S.-Y. Teow, S.-C. Peh, S.E. Mohamad, S.H. M. Taib, Green fabrication of biologically active magnetic core-shell Fe₃O₄/Au nanoparticles and their potential anticancer effect, *Mater. Sci. Eng.* 96 (2019) 51–57.
- [98] A. Gholobi, Z. Meshkat, K. Abnous, M. Ghayour-Mobarhan, M. Ramezani, F. H. Shandiz, K. Verma, M. Darroudi, Biopolymer-mediated synthesis of Fe₃O₄ nanoparticles and investigation of their in vitro cytotoxicity effects, *J. Mol. Struct.* 1141 (2017) 594–599.
- [99] Y.P. Yew, K. Shameli, S.E.B. Mohamad, Y. Nagao, S.-Y. Teow, K.X. Lee, E.D.M. Isa, Potential anticancer activity of protocatechuic acid loaded in montmorillonite/Fe₃O₄ nanocomposites stabilized by seaweed Kappaphycus alvarezii, *Int. J. Pharmaceut.* 572 (2019), 118743.
- [100] F. Barahuie, M.Z. Hussein, S. Abd Gani, S. Fakurazi, Z. Zainal, Synthesis of protocatechuic acid-zinc/aluminum-layered double hydroxide nanocomposite as an anticancer nanodelivery system, *J. Solid State Chem.* 221 (2015) 21–31.
- [101] B. Saifullah, K. Buskaran, R.B. Shaikh, F. Barahuie, S. Fakurazi, M.A. Mohd Moklas, M.Z. Hussein, Graphene oxide-PEG-protocatechuic acid nanocomposite formulation with improved anticancer properties, *Nanomaterials* 8 (2018) 820.
- [102] V. Ramalingam, M. Harshavardhan, S.D. Kumar, Wet chemical mediated hematite α -Fe₂O₃ nanoparticles synthesis: preparation, characterization and anticancer activity against human metastatic ovarian cancer, *J. Alloys Compound.* 834 (2020), 155118.
- [103] D. Zhi, T. Yang, J. Yang, S. Fu, S. Zhang, Targeting strategies for superparamagnetic iron oxide nanoparticles in cancer therapy, *Acta Biomater.* 102 (2020) 13–34.
- [104] A. Saranya, A. Thamer, K. Ramar, A. Priyadharsan, V. Raj, K. Murugan, A. Murad, P. Maheshwaran, Facile one pot microwave-assisted green synthesis of Fe2O3/Ag nanocomposites by phytoreduction: potential application as sunlight-driven photocatalyst, antibacterial and anticancer agent, *J. Photochem. Photobiol. B* 207 (2020), 111885.
- [105] D. Hariharan, P. Thangamuniandy, P. Selvakumar, U. Devan, A. Pugazhendhi, R. VasanthaJaya, L. Nehru, Green approach synthesis of Pd@TiO₂ nanoparticles: characterization, visible light active picric acid degradation and anticancer activity, *Pro. Biochem.* 87 (2019) 83–88.
- [106] P. Babji, D.R. Sri, Synthesis, characterization and antitumor activity of Fe₂O₃-Cu₂O-TiO₂ nanocomposite on MCF-7 human breast cancer cells, *J. Chem. Chem. Sci.* 6 (2016) 616–623.
- [107] V. Vignesh, G. Sathiyaranayanan, G. Sathishkumar, K. Parthiban, K. Sathish-Kumar, R. Thirumurugan, Formulation of iron oxide nanoparticles using exopolysaccharide: evaluation of their antibacterial and anticancer activities, *RSC Adv.* 5 (2015) 27794–27804.
- [108] Y.-T. Chen, Q. Yuan, L.-T. Shan, M.-A. Lin, D.-Q. Cheng, C.-Y. Li, Antitumor activity of bacterial exopolysaccharides from the endophyte *Bacillus amyloliquefaciens* sp. isolated from *Ophiopogon japonicus*, *Oncol. Lett.* 5 (2013) 1787–1792.
- [109] R. Kumar, M. Nayak, G.C. Sahoo, K. Pandey, M.C. Sarkar, Y. Ansari, V.N.R. Das, R. K. Topno, M. Madhukar Bhawna, P. Das, Iron oxide nanoparticles based antiviral activity of H1N1 influenza A virus, *J. Infect. Chemoth* 25 (2019) 325–329.
- [110] A. Cavezzì, E. Troiani, S. Corrao, COVID-19: Hemoglobin, Iron, and Hypoxia beyond Inflammation, *Narr. Rev. Clinin. Pract.* 10 (2020) 24–30.
- [111] Y. Yao, S. Miao, S. Yu, L.P. Ma, H. Sun, S. Wang, Fabrication of Fe₃O₄/SiO₂ core/shell nanoparticles attached to graphene oxide and its use as an adsorbent, *J. Colloid Interf. Sci.* 379 (2012) 20–26.
- [112] S.R. Kumar, M. Paulpandi, M. ManivelRaja, D. Mangalaraj, C. Viswanathan, S. Kannan, N. Ponpandian, An in vitro analysis of H1N1 viral inhibition using polymer coated superparamagnetic Fe3O4 nanoparticles, *RSC Adv.* 4 (2014) 13409–13418.
- [113] K. Ishihara, K. Fukumoto, Y. Iwasaki, N. Nakabayashi, Modification of polysulfone with phospholipid polymer for improvement of the blood compatibility. Part 1. Surface characterization, *Biomaterials* 20 (1999) 1545–1551.
- [114] Y. Mori, T. Ono, Y. Miyahira, V.Q. Nguyen, T. Matsui, M. Ishihara, Antiviral activity of silver nanoparticle/chitosan composites against H1N1 influenza A virus, *Nanoscale Res. Lett.* 8 (2013) 93.
- [115] L. Bromberg, D.J. Bromberg, T.A. Hatton, I. Bandín, A. Concheiro, C. Alvarez-Lorenzo, Antiviral properties of polymeric azidine- and biguanide-modified core-shell magnetic nanoparticles, *Langmuir* 28 (2012) 4548–4558.
- [116] F. Pinto, J.Y. Maillard, S.P. Denyer, P. McGeechan, Polyhexamethylene biguanide exposure leads to viral aggregation, *J. Appl. Microbiol.* 108 (2010) 1880–1888.
- [117] F. Pinto, J.Y. Maillard, S.P. Denyer, Effect of surfactants, temperature, and sonication on the virucidal activity of polyhexamethylene biguanide against the bacteriophage MS2, *Am. J. Infect. Control.* 38 (2010) 393–398.
- [118] J.G. Atherton, S.S. Bell, Adsorption of viruses on magnetic particles—II. Degradation of MS2 bacteriophage by adsorption to magnetite, *Water Res.* 17 (1983) 949–953.
- [119] J. McCullough, Progress toward a pathogen-free blood supply, *Clinical Infect. Dis.* 37 (2003) 88–95.
- [120] L. Gao, J. Zhuang, L. Nie, J. Zhang, Y. Zhang, N. Gu, T. Wang, J. Feng, D. Yang, S. Perrett, X. Yan, Intrinsic peroxidase-like activity of ferromagnetic nanoparticles, *Nat. Nanotechnol.* 2 (2007) 577–583.
- [121] T. Qin, R. Ma, Y. Yin, X. Miao, S. Chen, K. Fan, J. Xi, Q. Liu, Y. Gu, Y. Yin, J. Hu, X. Liu, D. Peng, L. Gao, Catalytic inactivation of influenza virus by iron oxide nanzyme, *Theranostics* 9 (2019) 6920–6935.

- [122] D.W. Coyne, Ferumoxytol for treatment of iron deficiency anemia in patients with chronic kidney disease, *Expert. Opin. Pharmacoth.* 10 (2009) 2563–2568.
- [123] Y. Abo-Zeid, N.S.M. Ismail, G.R. McLean, N.M. Hamdy, A molecular docking study repurposes FDA approved iron oxide nanoparticles to treat and control COVID-19 infection, *Eur. J. Pharm. Sci.* 153 (2020), 105465.
- [124] H.E.A. Mohamed, S. Afridi, A.T. Khalil, M. Ali, T. Zohra, M. Salman, A. Ikram, Z. K. Shinwari, M. Maaza, Bio-redox potential of Hyphaene thebaica in bio-fabrication of ultrafine maghemite phase iron oxide nanoparticles (Fe_2O_3 NPs) for therapeutic applications, *Mater. Sci. Eng.* 112 (2020), 110890.
- [125] N. Delaviz, P. Gill, A. Ajami, M. Aarabi, Aptamer-conjugated magnetic nanoparticles for the efficient removal of HCV particles from human plasma samples, *RSC Adv.* 5 (2015) 79433–79439.
- [126] T.N.L. Nguyen, T.V. Do, T.V. Nguyen, P.H. Dao, A.H. Nguyen, D.A. Dinh, T. A. Nguyen, T.K.A. Vo, T.L. Le, Antimicrobial activity of acrylic polyurethane/ Fe_3O_4 -Ag nanocomposite coating, *Prog. Org. Coat.* 132 (2019) 15–20.
- [127] T.D. Ngo, T.M.H. Le, T.V. Nguyen, T.A. Nguyen, T.L. Le, T.T. Nguyen, T.T.V. Tran, T.B.T. Le, N.H. Doan, Antibacterial nanocomposites based on Fe_3O_4 -Ag hybrid nanoparticles and natural rubber-polyethylene blends, *Int. J. Polym. Sci.* (2016), 2016.
- [128] R. Kunkalekar, M. Naik, S. Dubey, A. Salker, Antibacterial activity of silver-doped manganese dioxide nanoparticles on multidrug-resistant bacteria, *J. Chem. Technol. Biotechnol.* 88 (2013) 873–877.
- [129] P.N. Tri, T.A. Nguyen, T.H. Nguyen, P. Carriere, Antibacterial behavior of hybrid nanoparticles. Noble Metal-Metal Oxide Hybrid Nanoparticles, Elsevier, 2019, pp. 141–155.
- [130] S. Dacryor, M. Moussa, G. Turky, S. Kamel, In situ synthesis of Fe_3O_4 @ cyanoethyl cellulose composite as antimicrobial and semiconducting film, *Carbohyd. Polym.* 236 (2020), 116032.
- [131] S. Dacryor, H. Abou-Yousef, R.E. Abouzeid, S. Kamel, M.S. Abdel-Aziz, M. El-Badry, Antimicrobial cellulosic hydrogel from olive oil industrial residue, *Int. J. Biol. Macromol.* 117 (2018) 179–188.
- [132] Y. Prabhu, K.V. Rao, B.S. Kumar, V.S.S. Kumar, T. Pavani, Synthesis of Fe_3O_4 nanoparticles and its antibacterial application, *Int. Nano Lett.* 5 (2015) 85–92.
- [133] S. Mirsadeghi, H. Zandavar, M. Yousefi, H.R. Rajabi, S.M. Pourmortazavi, Green-photodegradation of model pharmaceutical contaminations over biogenic Fe_3O_4 /Au nanocomposite and antimicrobial activity, *J. Environ. Manag.* 270 (2020), 110831.
- [134] D.K. Padhi, T.K. Panigrahi, K. Parida, S. Singh, P. Mishra, Green synthesis of Fe_3O_4 /RGO nanocomposite with enhanced photocatalytic performance for Cr (VI) reduction, phenol degradation, and antibacterial activity, *ACS Sust. Chem. Eng.* 5 (2017) 10551–10562.
- [135] C. Lee, J.Y. Kim, W.I. Lee, K.L. Nelson, J. Yoon, D.L. Sedlak, Bactericidal effect of zero-valent iron nanoparticles on *Escherichia coli*, *Environ. Sci. Technol.* 42 (2008) 4927–4933.
- [136] P. Rana, S. Sharma, R. Sharma, K. Banerjee, Apple pectin supported superparamagnetic (γ - Fe_2O_3) maghemite nanoparticles with antimicrobial potency, *Mater. Sci. Energy Technol.* 2 (2019) 15–21.
- [137] M. Arshad, M. Abbas, S. Ehtisham-ul-Haque, M.A. Farrukh, A. Ali, H. Rizvi, G. A. Soomro, A. Ghaffar, M. Yameen, M. Iqbal, Synthesis and characterization of SiO_2 doped Fe_2O_3 nanoparticles: photocatalytic and antimicrobial activity evaluation, *J. Mol. Struct.* 1180 (2019) 244–250.
- [138] G.P. Halliah, K. Alagappan, A.B. Sairam, Synthesis, characterization of $\text{CH}-\alpha$ - Fe_2O_3 nanocomposite and coating on cotton silk for antibacterial and UV spectral studies, *J. Indust. Text.* 44 (2014) 275–287.
- [139] M. Raghu, K.Y. Kumar, M. Prashanth, B. Prasanna, R. Vinuth, C.P. Kumar, Adsorption and antimicrobial studies of chemically bonded magnetic graphene oxide- Fe_3O_4 nanocomposite for water purification, *J. Water Pro. Eng.* 17 (2017) 22–31.
- [140] G.J. Tortora, B.R. Funke, C.L. Case, D. Weber, W. Bair, Microbiology: an introduction, Benjamin Cummings, San Francisco, CA, 2004.
- [141] S.I. Siddiqui, S.A. Chaudhry, Nanohybrid composite Fe_2O_3 - ZrO_2 /BC for inhibiting the growth of bacteria and adsorptive removal of arsenic and dyes from water, *J. Cleaner Prod.* 223 (2019) 849–868.
- [142] S.I. Siddiqui, S.A. Chaudhry, A review on graphene oxide and its composites preparation and their use for the removal of As^{3+} and As^{5+} from water under the effect of various parameters: application of isotherm, kinetic and thermodynamics, *Procee. Saf. Environ. Protect.* 119 (2018) 138–163.
- [143] N.M. Sufya, R.W. Walli, F.M. Wali, M.S. Alareiba, B.M. Doro, Studies of the antimicrobial activity of Black Seed Oil from *Nigella Sativa*on *Staphylococcus aureus* and *Escherichia coli*, *Libyan J. Med. Res.* 8 (2014) 59–68.
- [144] M. Arakha, S. Pal, D. Samantarrai, T.K. Panigrahi, B.C. Mallick, K. Pramanik, B. Mallick, S. Jha, Antimicrobial activity of iron oxide nanoparticle upon modulation of nanoparticle-bacteria interface, *Scient. Rep.* 5 (2015) 1–12.
- [145] N. Tran, A. Mir, D. Mallik, A. Sinha, S. Nayar, T.J. Webster, Bactericidal effect of iron oxide nanoparticles on *Staphylococcus aureus*, *Int. J. Nanomed.* 5 (2010) 277.
- [146] N. Gao, Y. Chen, J. Jiang, Ag@ Fe_2O_3 -GO nanocomposites prepared by a phase transfer method with long-term antibacterial property, *ACS Appl. Mater. Interf.* 5 (2013) 11307–11314.
- [147] N. Madubuonu, S.O. Aisida, A. Ali, I. Ahmad, T.-k. Zhao, S. Botha, M. Maaza, F. I. Ezema, Biosynthesis of iron oxide nanoparticles via a composite of *Psidium guajava*-*Moringa oleifera* and their antibacterial and photocatalytic study, *J. Photochem. Photobiol. B* 199 (2019), 111601.
- [148] C. Das, S. Sen, T. Singh, T. Ghosh, S.S. Paul, T.W. Kim, S. Jeon, D.K. Maiti, J. Im, G. Biswas, Green synthesis, characterization and application of natural product coated magnetite nanoparticles for wastewater treatment, *Nanomaterials* 10 (2020) 1615.
- [149] Q. Li, C. Yong, W. Cao, X. Wang, L. Wang, J. Zhou, X. Xing, Fabrication of charge reversible graphene oxide-based nanocomposite with multiple antibacterial modes and magnetic recyclability, *J. Colloid. Interf. Sci.* 511 (2018) 285–295.
- [150] S. Qasim, A. Zafar, M.S. Saif, Z. Ali, M. Nazar, M. Waqas, A.U. Haq, T. Tariq, S. G. Hassan, F. Iqbal, Green synthesis of iron oxide nanorods using *Withania coagulans* extract improved photocatalytic degradation and antimicrobial activity, *J. Photochem. Photobiol. B* 204 (2020), 111784.
- [151] S. Parveen, A.H. Wani, M.A. Shah, H.S. Devi, M.Y. Bhat, J.A. Koka, Preparation, characterization and antifungal activity of iron oxide nanoparticles, *Microb. Pathog.* 115 (2018) 287–292.
- [152] S.M. Mandal, W.F. Porto, D. De, A. Phule, S. Korpole, A.K. Ghosh, S.K. Roy, O. L. Franco, Screening of serine protease inhibitors with antimicrobial activity using iron oxide nanoparticles functionalized with dextran conjugated trypsin and in silico analyses of bacterial serine protease inhibition, *Analyst* 139 (2014) 464–472.
- [153] S. Saqib, M.F.H. Munis, W. Zaman, F. Ullah, S.N. Shah, A. Ayaz, M. Farooq, S. Bahadur, Synthesis, characterization and use of iron oxide nano particles for antibacterial activity, *Micro. Res. Techniq.* 82 (2019) 415–420.
- [154] I.K. Herrmann, M.J.A. Wood, G. Fuhrmann, Extracellular vesicles as a next-generation drug delivery platform, *Nat. Nanotechnol.* (2021) 1–12.
- [155] Y.S.R. Krishnaiyah, V. Satyanarayana, B. Dinesh Kumar, R.S. Karthikeyan, In vitro drug release studies on guar gum-based colon targeted oral drug delivery systems of 5-fluorouracil, *Euro. J. Pharmaceut. Sci.* 16 (2002) 185–192.
- [156] N.R. Nelson, J.D. Port, M.K. Pandey, Use of superparamagnetic iron oxide nanoparticles (SPIONs) via multiple imaging modalities and modifications to reduce cytotoxicity: an educational review, *J. Nanotheranost.* 1 (2020) 105–135.
- [157] T. Vangijegem, D. Stanicki, S. Laurent, Magnetic iron oxide nanoparticles for drug delivery: applications and characteristics, *Exp. Opin. Drug Deliv.* 16 (2019) 69–78.
- [158] S. Zhao, X. Yu, Y. Qian, W. Chen, J. Shen, Multifunctional magnetic iron oxide nanoparticles: an advanced platform for cancer theranostics, *Theranostics* 10 (2020) 6278.
- [159] T. Skorjanc, F. Benyettou, J.C. Olsen, A. Trabolsi, Design of organic macrocycle-modified iron oxide nanoparticles for drug delivery, *Chem.–A Europ. J.* 23 (2017) 8333–8347.
- [160] P.H.-L. Tran, T.T.-D. Tran, T.V. Vo, B.-J. Lee, Promising iron oxide-based magnetic nanoparticles in biomedical engineering, *Arch. Pharm. Res.* 35 (2012) 2045–2061.
- [161] K. El-Boubbou, Magnetic iron oxide nanoparticles as drug carriers: preparation, conjugation and delivery, *Nanomedicine* 13 (2018) 929–952.
- [162] C. Sun, C. Fang, Z. Stephen, O. Veiseh, S. Hansen, D. Lee, R.G. Ellenbogen, J. Olson, M. Zhang, Tumor-targeted drug delivery and MRI contrast enhancement by chlorotoxin-conjugated iron oxide nanoparticles, *Nanomedicine (London, England)* 3 (2008) 495–505.
- [163] M.J. Jeon, C.H. Ahn, H. Kim, I.J. Chung, S. Jung, Y.H. Kim, H. Youn, J.W. Chung, Y.I. Kim, The intratumoral administration of ferucarbotran conjugated with doxorubicin improved therapeutic effect by magnetic hyperthermia combined with pharmacotherapy in a hepatocellular carcinoma model, *J. Exp. Clinical Cancer Res.* 33 (2014) 57.
- [164] D.H. Kim, Y. Guo, Z. Zhang, D. Procissi, J. Nicolai, R.A. Omary, A.C. Larson, Temperature-sensitive magnetic drug carriers for concurrent gemcitabine chemohyperthermia, *Adv. Healthcare Mater.* 3 (2014) 714–724.
- [165] J. Lee, H. Kim, S. Kim, H. Lee, J. Kim, N. Kim, H.J. Park, E.K. Choi, J.S. Lee, C. Kim, A multifunctional mesoporous nanocontainer with an iron oxide core and a cyclodextrin gatekeeper for an efficient theranostic platform, *J. Mater. Chem.* 22 (2012) 14061–14067.
- [166] S. Laurent, A.A. Saei, S. Behzadi, A. Panahifar, M. Mahmoudi, Superparamagnetic iron oxide nanoparticles for delivery of therapeutic agents: opportunities and challenges, *Expert Opin. Drug. Deliv.* 11 (2014) 1449–1470.
- [167] N. Kohler, C. Sun, J. Wang, M. Zhang, Methotrexate-modified superparamagnetic nanoparticles and their intracellular uptake into human cancer cells, *Langmuir* 21 (2005) 8858–8864.
- [168] R. Tong, L. Tang, L. Ma, C. Tu, R. Baumgartner, J. Cheng, Smart chemistry in polymeric nanomedicine, *Chem. Soc. Rev.* 43 (2014) 6982–7012.
- [169] G.Y. Lee, W.P. Qian, L. Wang, Y.A. Wang, C.A. Staley, M. Satpathy, S. Nie, H. Mao, L. Yang, Theranostic nanoparticles with controlled release of gemcitabine for targeted therapy and MRI of pancreatic cancer, *ACS Nano* 7 (2013) 2078–2089.
- [170] M.H. El-Dakdouki, D.C. Zhu, K. El-Boubbou, M. Kamat, J. Chen, W. Li, X. Huang, Development of multifunctional hyaluronan-coated nanoparticles for imaging and drug delivery to cancer cells, *Biomacromolecules* 13 (2012) 1144–1151.
- [171] Y. Wang, H.Z. Jia, K. Han, R.X. Zhuo, X.Z. Zhang, Theranostic magnetic nanoparticles for efficient capture and in situ chemotherapy of circulating tumor cells, *J. Mater. Chem. B* 1 (2013) 3344–3352.
- [172] X. Ding, Y. Liu, J. Li, Z. Luo, Y. Hu, B. Zhang, J. Liu, J. Zhou, K. Cai, Hydrazone-bearing PMMA-functionalized magnetic nanocubes as pH-responsive drug carriers for remotely targeted cancer therapy in vitro and in vivo, *ACS Appl. Mater. Interfaces* 6 (2014) 7395–7407.
- [173] L. Zhu, D. Wang, X. Wei, X. Zhu, J. Li, C. Tu, Y. Su, J. Wu, B. Zhu, D. Yan, Multifunctional pH-sensitive superparamagnetic iron-oxide nanocomposites for targeted drug delivery and MR imaging, *J. Control. Release* 169 (2013) 228–238.
- [174] Z. Zhao, D. Huang, Z. Yin, X. Chi, X. Wang, J. Gao, Magnetite nanoparticles as smart carriers to manipulate the cytotoxicity of anticancer drugs: magnetic control and pH-responsive release, *J. Mater. Chem.* 22 (2012) 15717–15725.

- [175] M.-Y. Hua, H.-W. Yang, C.-K. Chuang, R.-Y. Tsai, W.-J. Chen, K.-L. Chuang, Y.-H. Chang, H.-C. Chuang, S.-T. Pang, Magnetic-nanoparticle-modified paclitaxel for targeted therapy for prostate cancer, *Biomaterials* 31 (2010) 7355–7363.
- [176] H.-W. Yang, M.-Y. Hua, H.-L. Liu, R.-Y. Tsai, C.-K. Chuang, P.-C. Chu, P.-Y. Wu, Y.-H. Chang, H.-C. Chuang, K.-J. Yu, Cooperative dual-activity targeted nanomedicine for specific and effective prostate cancer therapy, *ACS Nano* 6 (2012) 1795–1805.
- [177] C. Ansari, G.A. Tikhomirov, S.H. Hong, R.A. Falconer, P.M. Loadman, J.H. Gill, R. Castaneda, F.K. Hazard, L. Tong, O.D. Lenkov, D.W. Felsher, J. Rao, H. E. Daldrup-Link, Development of novel tumor-targeted theranostic nanoparticles activated by membrane-type matrix metalloproteinases for combined cancer magnetic resonance imaging and therapy, *Small (Weinheim an der Bergstrasse, Germany)* 10 (2014) 566–575, 417.
- [178] X. Li, M. Zhen, R. Deng, T. Yu, J. Li, Y. Zhang, T. Zou, Y. Zhou, Z. Lu, M. Guan, H. Xu, C. Shu, C. Wang, RF-assisted gadofullerene nanoparticles induces rapid tumor vascular disruption by down-expression of tumor vascular endothelial cadherin, *Biomaterials* 163 (2018) 142–153.
- [179] J.H. Gill, P.M. Loadman, S.D. Shnyder, P. Cooper, J.M. Atkinson, G. Ribeiro Morais, L.H. Patterson, R.A. Falconer, Tumor-targeted prodrug ICT2588 demonstrates therapeutic activity against solid tumors and reduced potential for cardiovascular toxicity, *Mol. Pharm.* 11 (2014) 1294–1300.
- [180] D. Turiel-Fernández, L. Gutiérrez-Romero, M. Corte-Rodríguez, J. Bettmer, M. Montes-Bayón, Ultrasmall iron oxide nanoparticles cisplatin (IV) prodrug nanoconjugate: ICP-MS based strategies to evaluate the formation and drug delivery capabilities in single cells, *Analy. Chim. Acta* 1159 (2021), 338356.